December 2015

Study of homogeneous mineral acid dehydration of monosaccharides in a CSTR

Siddharth Sharad Bhat
Syracuse University

Abstract

Simple sugars (Aldohexoses/pentoses), (Ketohexoses/pentose) when subjected to a dehydration reaction, produce various compounds. An example of one such compound is 5-hydroxymethyl furfural. Such chemical products may be used in subsequent processing steps (hydrolysis, aldol condensation, hydrogenation and dehydration) to produce similarly structured condensed compounds that form the basis of complex molecules used in various industries such as production of fuels, chemical reagents and fertilizers. Most studies focus on heterogeneous packed beds and batch reactors to carry out dehydration reactions. This study illustrates use of a Continuous Stirred-Tank reactor to carry out such dehydration reactions. In order to maintain the homogenous nature of the reaction, the catalyst chosen was sulfuric acid. Use of a CSTR would allow study of kinetics and yields for varying residence times. This data could be used to design large scale operations in biomass processing. This study is aimed at investigating variables such as changing physical properties of the fluid reactant during reaction, variation in pH and consequent change in proton concentrations. By understanding the impact of these variables, more accurate rate measurements can be made. In the process of developing the right method for data acquisition, several substantial changes were made to the reactor and methods. These changes were instrumental in development of a cyclic process of data collection and changing methods and design, thus highlighting the chemical engineering heuristics approach and refinement in processes. The sequence of corrected results give us better insight into the process and help develop accurate models for the reactions in the scope of this thesis and also future studies. The presented results of rates and yields may be used to develop processes based on requirement and feasibility.

STUDY OF HOMOGENEOUS MINERAL ACID DEHYDRATION OF MONOSACCHARIDES IN A CSTR

By

Siddharth Bhat
Mumbai University 2009-2013

THESIS

Submitted in partial fulfillment of the requirements for the
Degree of Master of Science in Chemical Engineering
In the Graduate School of Syracuse University

December 2015

Acknowledgements

I would like to thank my advisor, Professor Jesse Q. Bond for granting me the opportunity to learn and grow as a part of the lab. My journey through the Masters program has been especially memorable and enjoyable on account of the continued guidance and support I received. I am grateful to all the faculty members, administrative staff and workshop staff (Bill and Dick) that assisted me through these two years. I appreciate the time spent by Dr. Benjamin Akih Kumgeh, Dr. Shikha Nangia and Dr. Lawrence Tavlarides for taking the time to review my written thesis and for being a part my dissertation panel.

A special thank you is directed to my lab mates, especially Omar who designed the reactor setup I had the privilege of working on, for the time and effort he spent in guiding me through the basics of laboratory operations, Argy for his valuable advice. Thanks to Christian, Josh and Shoufau for always keeping it simple and fun.

Lastly, I would like to thank my entire family for their unconditional love and support through my education. I would like to dedicate the success of this thesis project to my parents, Sharad Bhat and Veena Bhat and to my girlfriend Niyati Shetty.

Table of Contents

A) Figures

Tables

Chapter I
Introduction

Crude oil has been the main feedstock for most of the chemical industry since the early 19th century. “Building block chemicals” in most chemical processing industries can be traced back to crude oil. An examination of products manufactured by way of petrochemical processing reveal our dependence on crude oil. Plastics and polymers, paints, fuels, reagents and chemical solvents are all petrochemical products. Although energy supplies may be supplemented through the use of solar power, wind turbines and geothermal sources, it is established that our only renewable source of carbon for chemical manufacture is biomass. Several sources and studies find that society can depend on the reserves of crude oil for several decades to come, however, the environmental repercussions of such dependence and the increasing demands of technological advances and population growth make current consumption patterns unsustainable [1-5]. New techniques of sourcing crude oil from “fracking” and subsequent processes have taken their toll on the environment. Several studies indicate that the use of biomass-derived fuels directly lessen emission impacts. Also, their large scale manufacture has a relatively smaller impact [6-9]. Although short term fuel price fluctuations may not indicate a long term shortage, depletion of crude oil reserves is inevitable (projected cost in the year 2025, $54 per barrel)[10].

The petrochemical industry was established in the early 20th century and has evolved to become very efficient and economical with regards to overall yields and conversions. We can make use of existing chemical engineering technologies (separation, hydrolysis, dehydration and pyrolysis, among others) to modify the existing refinery setup to operate on a different feedstock (Biomass Refinery) [10].

Selected biomass feeds may be used in the manufacture of specialty chemicals, pharmaceuticals, natural polymers and other higher value products. When we consider fuel

manufacture from biomass, an important constraint that needs to be managed is the heat content. Increasing the energy density is the primary focus in fuel technology. This requires the removal of oxygen as carbon dioxide and water. Some of the oxygen may be left behind in the interest of better combustion properties. Dehydration and hydrogenolysis are effective strategies used to reduce oxygen content of biomass[12.] In general, biomass is found to have approximately 45 wt% oxygen.

An important factor in changing manufacturing processes is maintaining economic feasibility of the process. Biomass may be sourced as a virgin biomass or waste biomass. Waste biomass consists of remnants of harvesting food crops, wastes from paper industry and wastes from sugar manufacture. Virgin biomass consists of crops or plants grown specifically for use in biomass processing. Virgin biomass brings into question the food versus fuels argument and so, efforts have been made to maximize waste biomass use in processing. Bioengineering can help to manipulate the growth patterns/requirements of these crops. Waste biomass in the form of landfill/industrial residues, paper pulp black liquor, cornstover may be used as a cheap feedstock, in some cases negative-cost. Waste energy content in the US amounts to a 15.1 EJ/year which is significant considering annual energy consumption of 41 EJ/year[3.]

Experts in the field predict that by the year 2030, 20% of transportation fuels and 25% of chemicals will come from biomass[10.]Most of the major petrochemical oil companies have identified this trend and have begun to develop technologies for biofuel and biochemical production[14-17.] So, how does biomass figure into the scheme of processing steps? To understand this we need to take a closer look first at the specific components of biomass.

Chapter II

Literature Review

2.1 Biomass

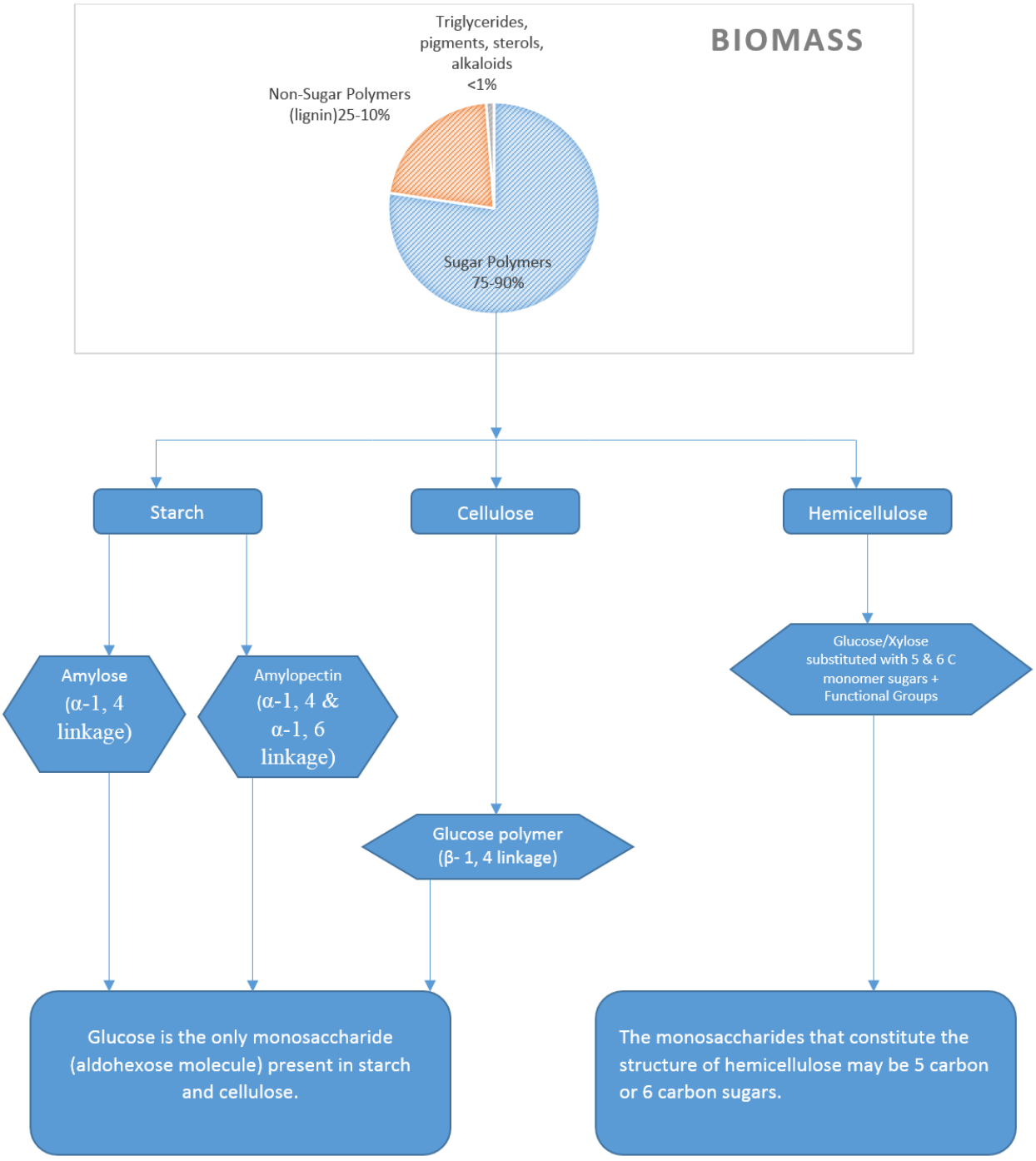

Figure 1: Composition of Biomass

All types of biomass originate from plant sources. Fixed carbon, light and water are converted to sugar in the photosynthesis reaction. Plant sugars are stored within plant cells in the form of sugar polymers. The nature and distribution of these polymers within the plant cell is a function of plant type. Bio engineering has been instrumental in manipulating this distribution to suit our requirements. Through gene manipulation, scientists have successfully increased cellulose distribution by reducing lignin in plant species while maintaining plant growth advantages[45.]

Figure 1 illustrates the distribution of different chemical species present in biomass. Biomass is primarily composed of 75-90% sugar polymers, 25-10% non-sugar polymers and approximately 1% triglycerides, sterols, pigments, alkaloids and other compounds. Biomass processing begins at the sugar polymers. Broadly speaking, sugar polymers may be present in the form of starch, cellulose or as hemicellulose. Cellulose is the most abundant biopolymer. It is a polymer of glucose with β- 1, 4 glycoside linkages[5.] The molecular weight of cellulose can range from 300,000 to 500,000 g/mol. This type of linkage renders cellulose crystalline. Glucose oligomers (dimers, trimers, tetramers etc.) are formed during partial hydrolysis of cellulose[46.] Glucose monomers are produced through complete hydrolysis of cellulose.[47] Hydrolysis of cellulose is relatively difficult owing to its crystallinity.

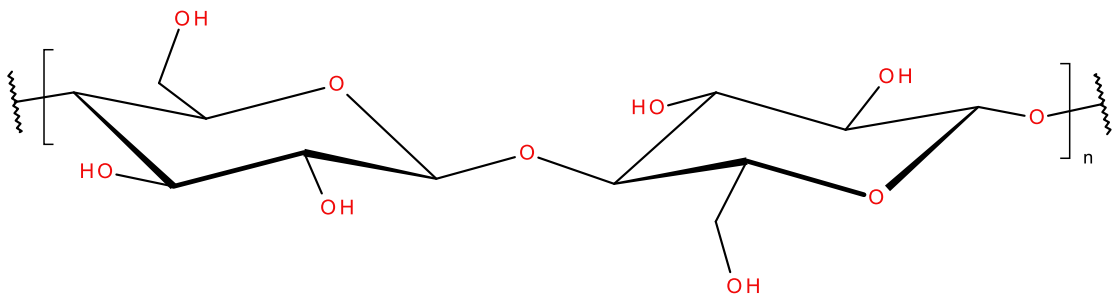

Figure 2: Structure of Cellulose

Hemicellulose is another branched sugar polymer. Depending on species, it consists of a branched glucose or xylose substituted with arabinose, xylose, galactose, fucose, mannose, glucose or gluconic acid. Side chains may also contain acetyl groups or ferulate[61.] Sugars in hemicellulose may contain either 5 carbon atoms or 6 carbon atoms. Xylose and arabinose are examples of the 5 carbon sugars while glucose, galactose and maltose are some 6-carbon sugars. In general, hemicelluloses, are easier to hydrolyze owing to amorphous nature.

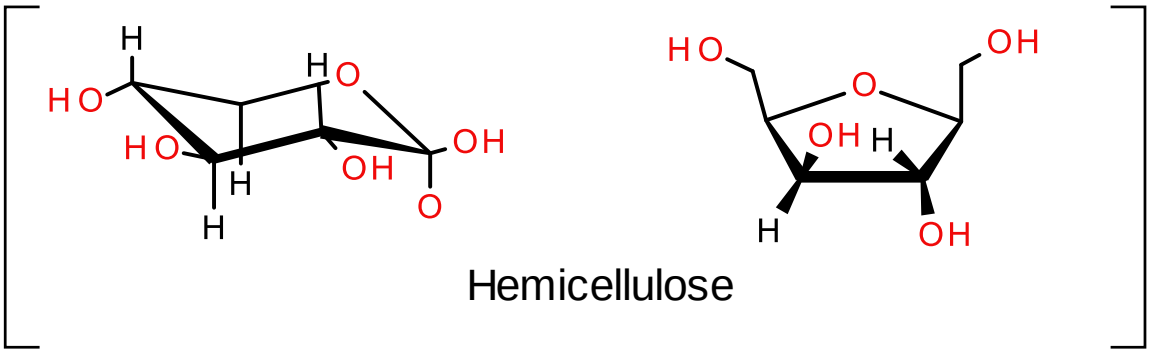

Figure 3: Components of Hemicellulose

Starch is made up of Amylose (10-20%) and Amylopectin (80-90%). Amylose and amylopectin are polymers of glucose. Amylose is water soluble due to its α-1, 4 glycoside linkages while Amylopectin is insoluble due to its combination of α-1, 4 glycoside linkage and α-1, 6 glycoside linkage[18.]

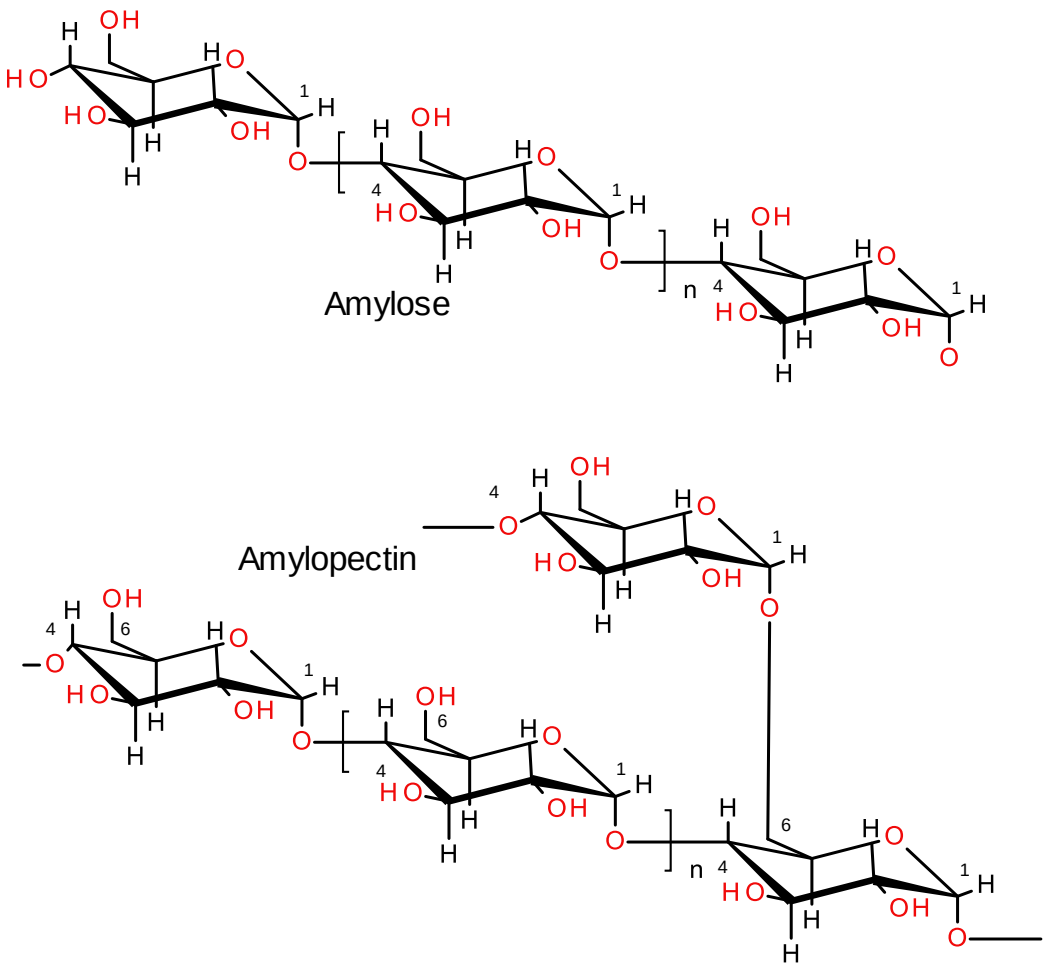

Figure 4: Components of Starch (Amylose and Amylopectin)

The monomers that form the fundamental building blocks of the sugar polymers may be classified into pentoses (5 carbon sugar monomer) or hexoses (6 carbon sugar monomers). Also, they may be functionally different (keto or aldehyde groups). Dehydration of these monomers produce the chemical molecules of interest to us. The reactions and products that these molecules generate are different. Pentose sugars produce furfural upon dehydration, while hexose sugars produce 5-hydroxymethyl furfural.

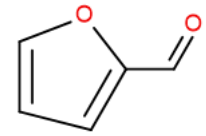

Furfural

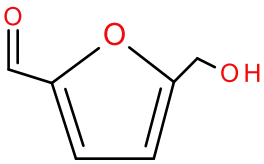

HMF

Figure 5: Structure of Furanic Aldehydes (Furfural and HMF)

The cellulose and hemicellulose found in plant cells are bound by lignin, they are collectively referred to as lignocellulose. $\sim 2 \times 10^{11}$ Metric tons of lignocellulose are available for processing[19]. Although lignocellulose does contain sugar polymers such as cellulose and hemicellulose, separating these polymers from the lignin is an energy intensive process and requires preprocessing steps[20]. Difficulty in processing lignocellulose arises on account of the crystalline nature of cellulose and protection by lignin. However, preprocessing of lignocellulose to cellulose and hemicellulose solves the age old "food vs fuel" argument[51]. Most remnants of food processing, such as cornstover may pass through preprocessing steps to yield useable products. Cornstover has a distribution of 27-48% cellulose, 13-17% hemicellulose 18-25% lignin[20]. In this case, the question of cultivating crops solely for fuel doesn't arise. At the same time, the uniform quality and desirable properties of feedstocks are maintained.

The non-sugar polymers are comprised of lignin. Lignin is a cross-linked phenolic polymer, which on de-polymerization yields aromatics. These compounds have a high heating value and are of a great economic significance. Research into effective lignin processing steps is underway [22-25].

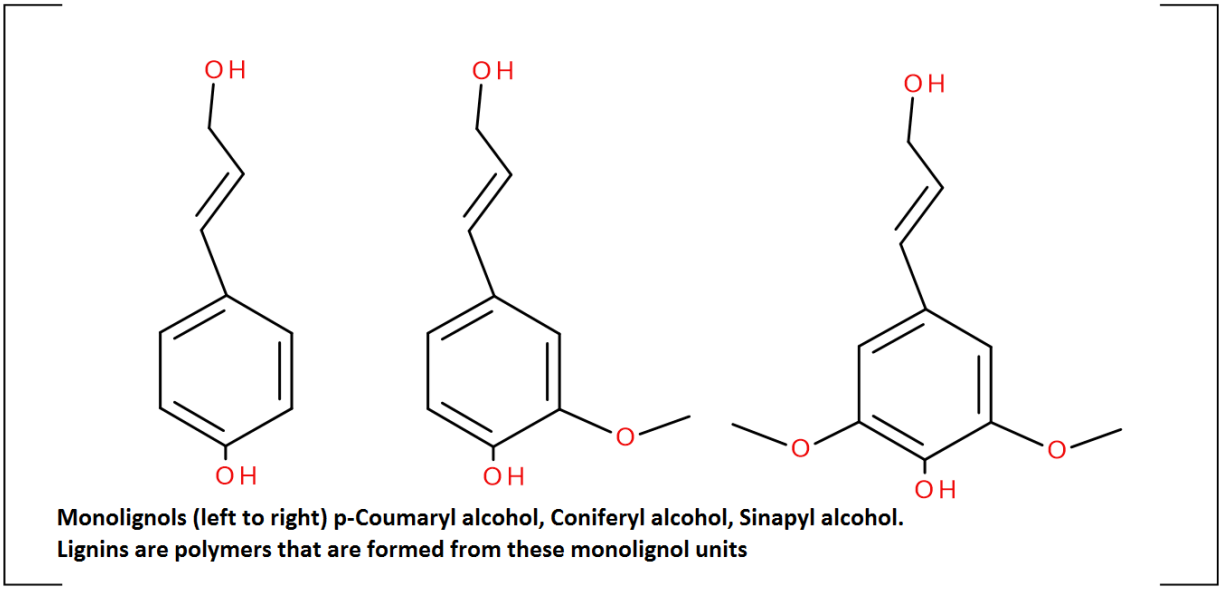

Figure 6: Structure of monolignol units

Dumesic found that a solvent derived from lignin could replace the organic phase solvents used in biphasic biomass reaction systems. Furanics (5-HMF, furfural) and lactones (GVL) could be extracted into the lignin derived phenolic solvent to make the process more sustainable.[26]

Three main routes may be taken to manufacture fuel compounds from biomass. This can be illustrated through the use of the following diagram.

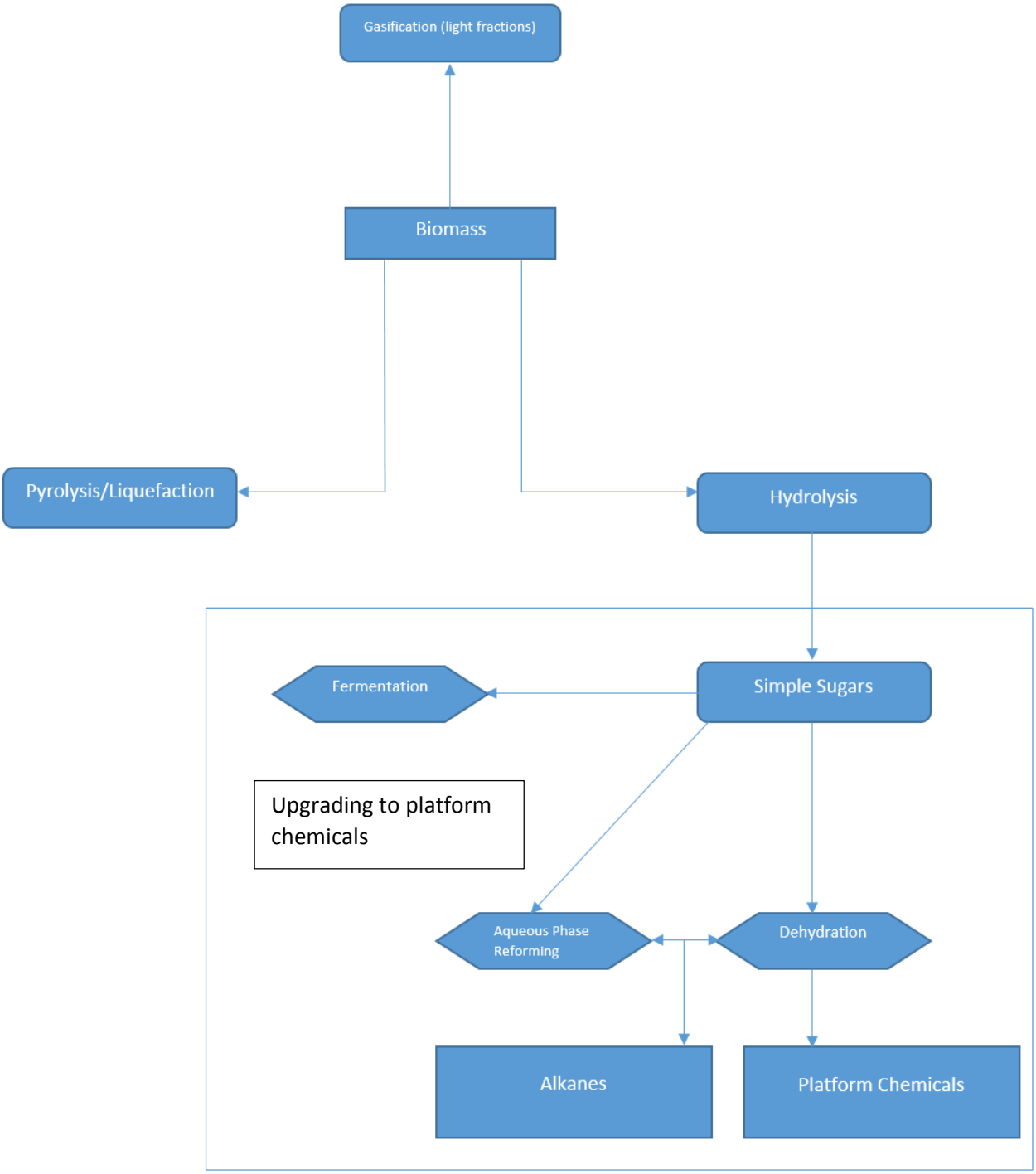

Figure 7: Biomass Processing/Upgrading routes

Gasification of biomass yields light fractions mostly with larger vapor pressures such as carbon monoxide, carbon dioxide, hydrogen, methane, trace amounts of higher hydrocarbons

such as ethane and ethene, water, nitrogen along with a few impurities depending upon the gasification methods. This stream may be used to produce methanol or in Fischer-Tropsch reactions to generate longer chain compounds that are of greater economic value. Pyrolysis and hydrolysis of biomass yield liquid fractions. Of these, pyrolysis yields heavier oils (bio-oil, pyrolysis oil), tars, acids and aromatics. These are then upgraded or processed to fuels. Hydrolysis is used to convert the sugar polymers into monomers of sugar. Hydrolysis may be carried out through the use of either microbial fermentation or acid reaction steps. After complete hydrolysis, we are left with monomers such as glucose, among the 6 carbon molecules and xylose, among the 5 carbon molecules.

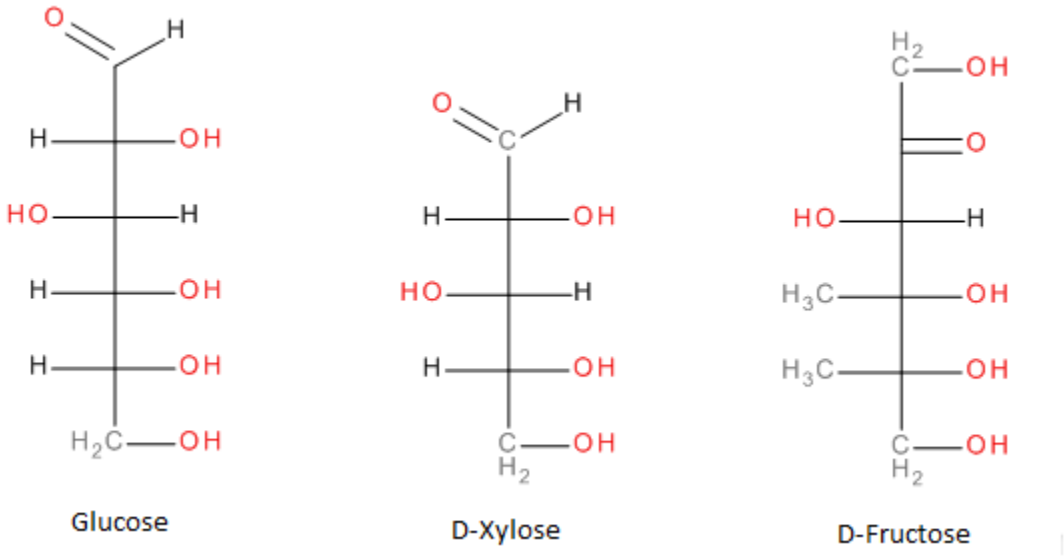

Figure 8: Sugar monomers Glucose, Fructose and Xylose

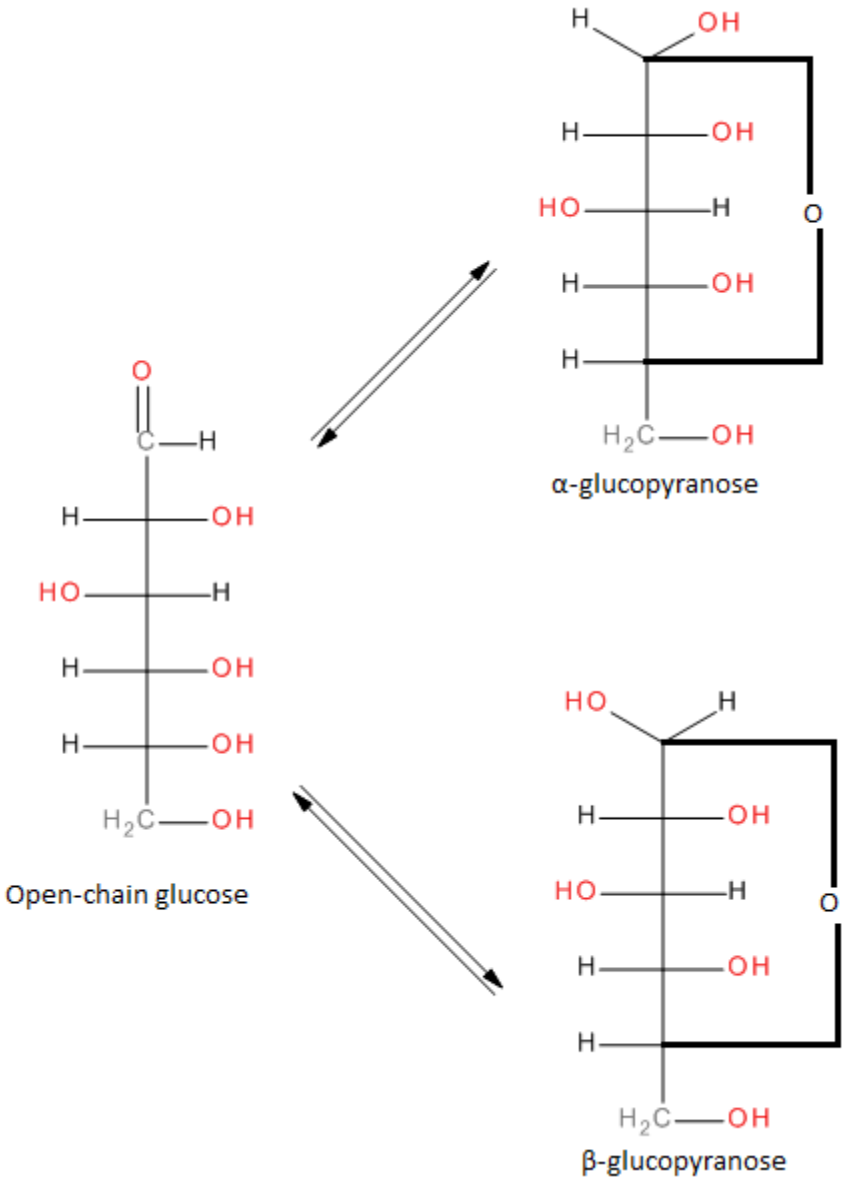

Figure 9: Fischer projections of open chain and closed chain forms of glucose.

Polyols exist in two forms, open chain form as shown on the left of Figure 9 and closed chain forms as illustrated on the right. When dissolved in water, there exists a temperature equilibrium dependent ratio of these two forms of the compound. Glucose, fructose and xylose exist in similar anomeric forms. Glucose and fructose solutions retain < 1% open chain or acyclic

form. Glucose solutions are found to contain a smaller ratio of acyclic to cyclic chain ratios than fructose [67.]

2.2 Upgrading Technologies

Once the simple sugars are produced, several conversion technologies may be used for further processing (upgrading). Some of these conversion technologies used are biological, thermal, chemical/catalytic upgrading or a combination of these technologies. Fermentation has been employed to convert coal and petroleum gas streams into ethanol[13.] Also, use of fermentation in processing biomass is an important application of microbial enzymatic technology. Sugarcane and other virgin biomass species are being used widely to produce ethanol from starches. Studies are being conducted on the use of lignocellulosic agricultural wastes as a feed in the fermentative process. For this reason, strains of bacteria that are adept at fermenting both glucose and xylose need to be studied [55, 56]. Also, since fermentation steps generally begin at simple sugar monomers, it is imperative to research combining enzymatic techniques of hydrolysis of starches (cellulose) and enzymatic fermentation. Fermentation quite often requires preprocessing steps to free the fermentable sugars. These preprocessing steps include ammonia explosion, aqueous ammonia recycle, controlled pH, dilute acid, flow through, and lime[58.] Glucose fermentation can be used to produce a range of products through recombinant or non-recombinant DNA technologies and through different pathways. Some of these products are mixed acids (acetic acid, succinic acid, propionic acid, butyric acid, lactic acid), alcohols (ethanol, butanol, isopropanol) and glycols with carbon dioxide. Each of these products can be used to manufacture useful products. Succinic acid for example can be used to

manufacture pharmaceuticals and biodegradable polymers. Succinic acid is a precursor to many industrially important chemicals such as adipic acid, 1, 4-butanediol, tetrahydrofuran (THF), N-methyl pyrrolidinone, 2-pyrrolidinone, gamma butyrolactone and succinate salts. Fermentation of waste biomass can be used to produce other products such as methane gas (biogas plants/waste sludge treatment) and hydrogen gas. Hydrogen gas can be used as a prospective green fuel through the use of fuel cells thereby producing water as a byproduct. Although these technologies of fermentation to produce hydrogen are only in the fledgling stages of development, certain anaerobic photosynthetic fermentative strains of bacteria have shown promise for their H_2 producing capability from glucose[57]. Fermentation does come with its share of limitations. In most cases, the fermentation microbes are mixed into the feed. Separation of the suspended microbes and the products of fermentation can be energy intensive. Use of immobilized growing species on substrates becomes extremely challenging. Dilute feed streams are required in most cases. Auxiliary batch operations are needed in some cases for yeast/bacteria cultivation. Once the hydrolysis step is achieved either enzymatically or through the use of acids, simple sugars are produced and made ready for the next step of the process. Assuming complete hydrolysis, simple sugars produced may be upgraded to platform chemicals.

Renewable energy research has been focused on ways of breaking down organic wastes into fundamental molecules and taking advantage of the functional properties to create raw material chemicals. This is the concept of platform chemicals. Several platform chemicals have been identified as useful building blocks for chemicals. These resulting compounds may be used as is, or in subsequent platform chemical manufacture. 5-HMF and furfural have been identified as platform chemicals. Dehydration of glucose, fructose and xylose to produce platform chemicals will be studied in the proceeding part of the study.

2.3 Acid Catalyzed Dehydration

Hexose sugars on triple dehydration yield HMF. The exact mechanism varies with regard to type of solvent used [32-35]. No definitive conclusion has been made on mechanism of hexose dehydration. Isomerization of glucose to fructose and vice-versa is a common factor between most studies. Side reactions form humins and organic acids like levulinic acid [36, 37]. Acids formed as a result of side reactions have been known to self-catalyze the reaction. Side reactions are affected by the solvent type, temperature and catalyst. Dehydration products are one of the four reaction products formed during decomposition of polyols. Isomerization, fragmentation and condensation also take place at elevated temperatures. Two mechanism schemes were proposed to explain dehydration of fructose and glucose. The first scheme suggests a series of reactions commencing with and retaining the fructofuranose ring or cyclic form of fructose. The second scheme postulates a succession of reactions proceeding mainly via open-chain or linear intermediates. Literature is in favor of the first scheme. Higher yields of HMF have been reported in dehydration studies of fructose [62-64]. Rates of HMF production and also selectivity was higher for fructose dehydration when compared to dehydration of glucose. Glucose is much cheaper and more widely available when compared to fructose. The catalytic pathway of glucose and fructose dehydration is shown in Figure 10. Glucose isomerizes to fructose or to form HMF.

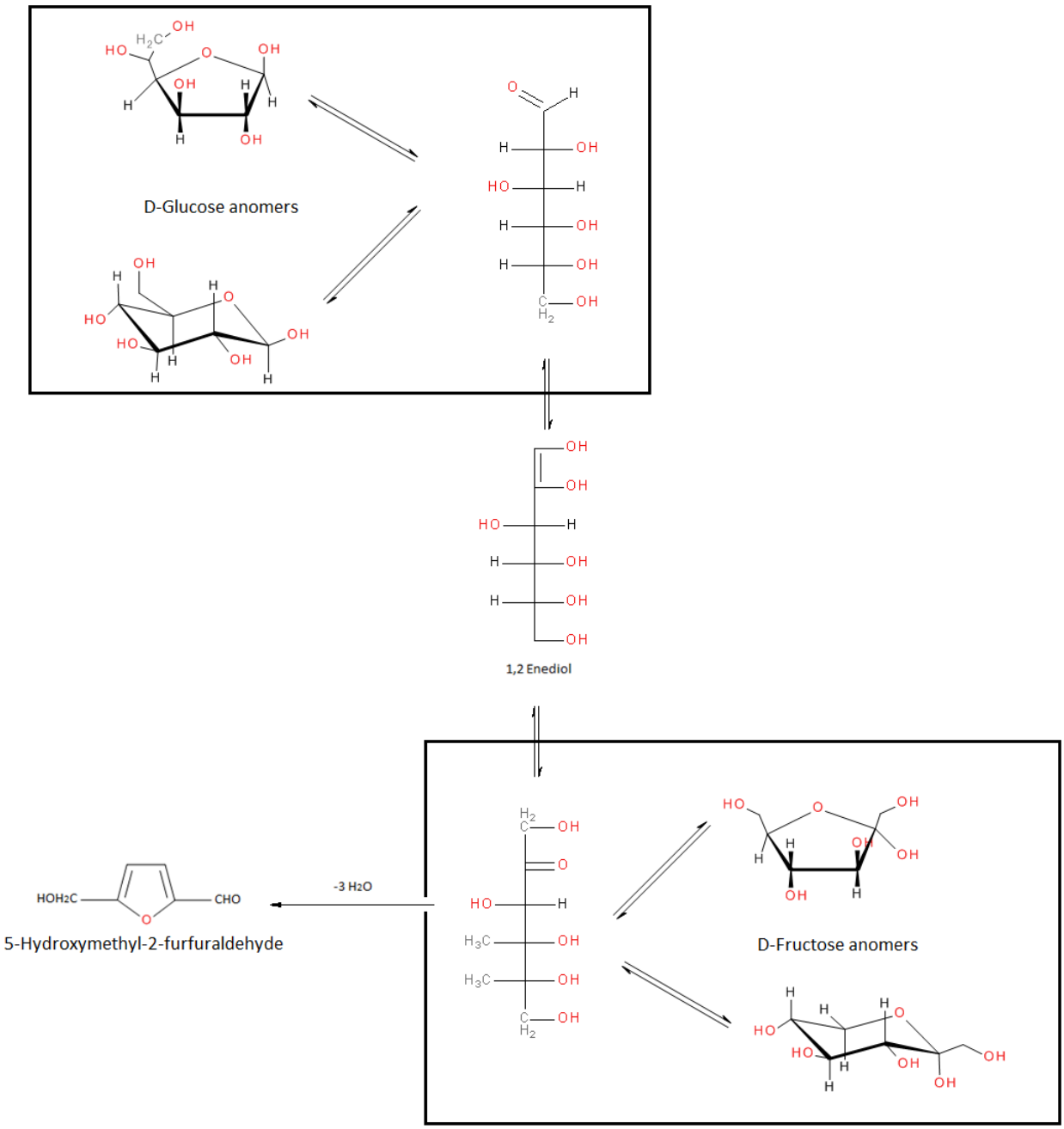

Figure 10: Postulated mechanism for the production of hydroxymethylfurfural (HMF) [68].

Biomass derived feed-stocks have low thermal stabilities and their functional groups are hydrophilic compared to their petrochemical counterparts. This makes aqueous phase processing a requirement in most of the reactions involving biomass. Early research into sugar chemistry

involved detailed models for kinetic studies of hydrolysis of starch[29]. These studies revealed that hydrolysis was accompanied by an undesired decomposition reaction. The product was HMF. Levulinic acid was formed as a result of acid catalyzed degradation of starch. It was only later realized that these products could be used in processing steps further to yield useful products. These reactions form an essential step in biomass processing. Dehydration may also be coupled with hydrogenation to carry out a set of reactions. These reactions form the basis of the biomass refinery. Aqueous phase dehydrations using mineral acids have been well documented and studied [3, 27, 28, 30]. Furanic aldehydes (HMF and furfural) may be upgraded to higher alkanes through a series of condensation reactions and hydrogenation/dehydration reactions[31].

2.4 Platform Chemicals
2.4.1 HMF

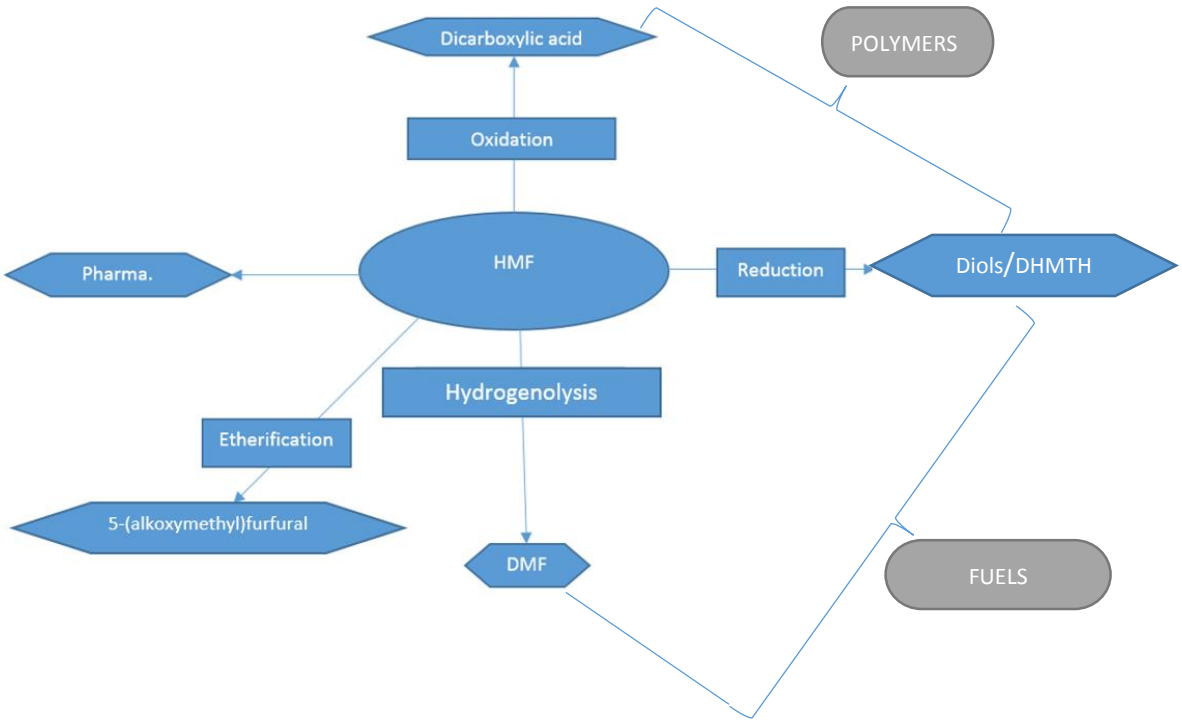

Figure 11: HMF as a platform chemical

HMF can be processed through different chemical processing steps to manufacture useful chemicals. The oxidation route produces dicarboxylic acid groups such as furan dicarboxylic acid FDCA which can be used to make products similar to the petrochemical product PET (poly ethylene terephthalate). Reduction of HMF produces dihydroxymethyl tetrahydrofuran DHMTHF which can be used to produce polymers as well as in the fuel industry as already explained in biomass refinery setup [38.] Hydrogenolysis of HMF also helps in fuel manufacture. Molecules such as dimethylfuran (DMF) are useful as fuel additives [39, 40]. Etherification of HMF yields ethers such as 5–alkoxymethylfurfuralether a useful intermediate in fuel industries [41, 42, 43]. The heterocyclic structure of furans is useful in manufacture of

biologically active compounds is an important intermediate for pharmaceutical industry. A series of hydrogenation, condensation and dehydration reactions may be employed to convert HMF into linear chain alkanes. Hydrogenation reactions help to saturate all the bonds in the compound. Aldol condensations increase the overall chain length and the final step in alkane production is a hydrogenation accompanied by the removal of water molecules to finally produce the required linear alkane. These series or reactions are manipulated depending upon the desired chain length of final alkane. It is possible to produce 7-15 carbon alkanes through combined use of HMF and furfural[31.]

2.4.2 Furfural

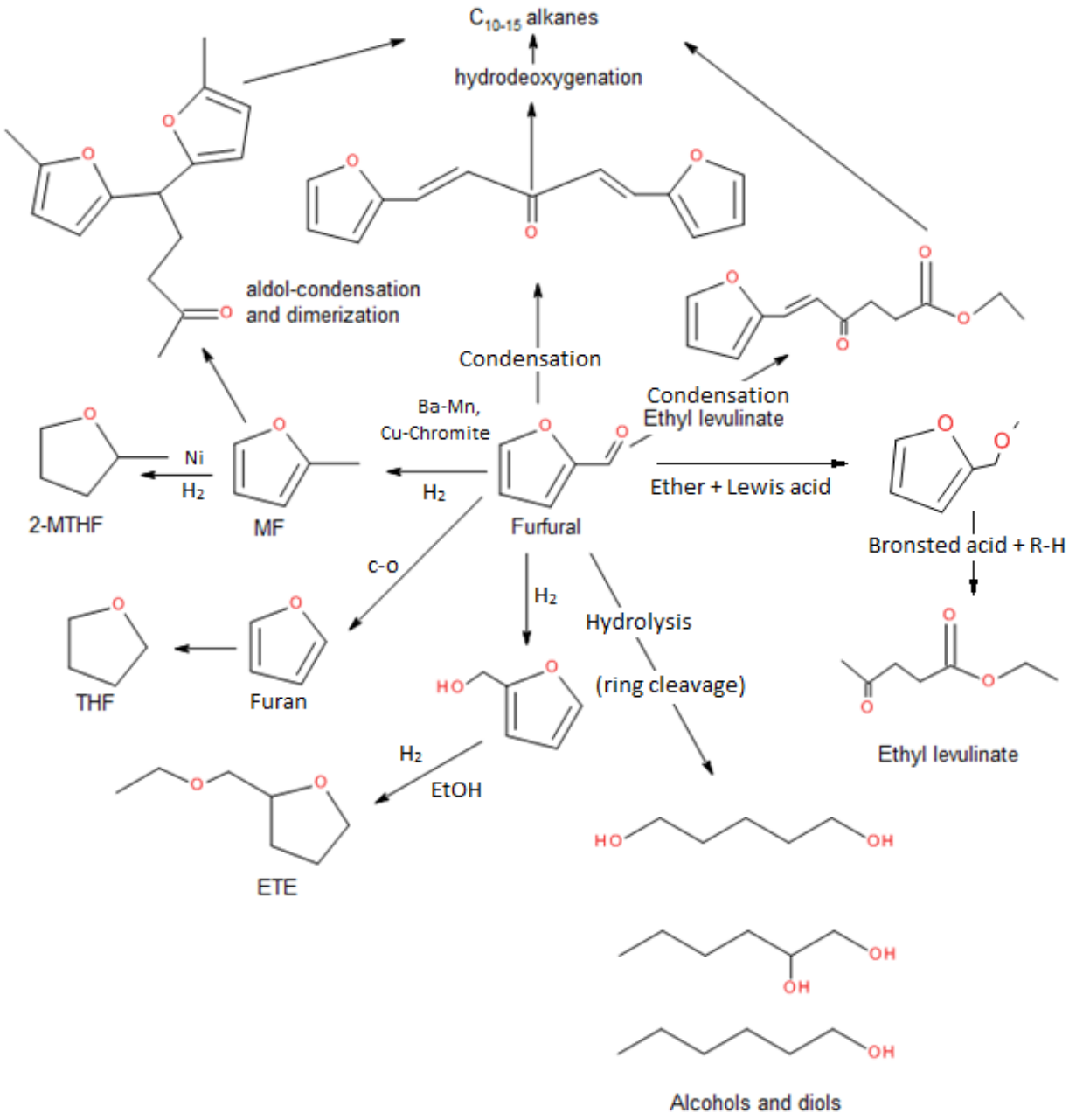

Figure 12: Furfural as a platform chemical [11.]

Furfural is being researched for a range of specialized chemical applications. Bisphenol-A-furfural a furfural based polymer resin has shown advantages over phenol-formaldehyde resins as regards thermal, chemical, physio-mechanical, and electrical properties[59.] Furfural may be used to manufacture solvents (methylfuran), furfuryl alcohol and furoic acid. Furfural and

hydrogen when fed through Ni or Ni-Fe SiO_2 bed, form furfuryl alcohol and furans. Hydrogenation reactions result in the formation of furfuryl alcohol which then may be hydrogenolyzed to yield 2-methyl furan. The furans produced in the Ni-Fe catalyzed bed may be used to produce 4 carbon compounds such as butanal, butanol and butane[60.] Hydrogenation steps to upgrade furfural into fuel compounds is still considered to be the more important conversions. Similar sequence steps used to convert HMF to linear alkanes may be used to convert furfural into desired alkanes. Special types of reactors are used for these reactions. These reactors consist of four phases. The aqueous inlet stream with water soluble organic content, the hexadecane solvent stream, a gas inlet H_2 and the solid catalyst (Pt/SiO_2-Al_2O_3). Since dehydration hydrogenation reactions take place in this four phase setup. This setup is referred to as a 4-PD/H reactor system[31.] Aldol coupling of furfural with levulinic acid can be seen in the top right of Figure 12.

2.5 Reaction Orders and Rate Law

In the experiments carried out, sugars were consumed (disappearing reactant). Rate depends on temperature and composition. "Rate r, is expressed as the product of rate constant, k, and concentrations of the reactant,

The rate constant, k, is a function of temperature, catalyst, ionic strength and solvent. For reacting species A and B

$$-r = kC_A^{\alpha}C_B^{\beta} \qquad \text{Equation 1}$$

The rate law involves the product of rate constant and reacting species concentrations with their respective exponents. In the case of our reactions of sugar and protons, we have,

$$-r = kC_{sugar}^{\alpha}C_{[H^+]}^{\beta} \qquad \text{Equation 2}$$

Rate data collected can be used to determine the activation energy and pre-exponential factors for the reaction. To be able to do so, we use the Arrhenius Equation.

$$k(T) = Ae^{-Ea/RT} \qquad \text{Equation 3}$$

The Arrhenius plot is a great way to extrapolate rate coefficient data for temperatures that have not been investigated. A in the above equation represents the pre-exponential factor, E_A is the activation energy, R is the gas constant (8.314 J/mol) and Temperature "T" is measured in degree Kelvin.

This study aims to calculate the rates, activation energy and pre-exponential factors for reactions with different sugars. By doing this, it is also possible to compare different catalysts for similar dehydration reactions. Just as increasing temperatures increase rate constants, changing catalysts may alter the nature and number of molecular collisions and increase rates. Reactions carried out at different temperatures yield different values of rate constant k. Plotting ln k as a

function of (1/T) yields a slope of –Ea/R. The Arrhenius equation may also be written in semi-log form as,

$$\ln k = lnA - \frac{E_a}{RT} \quad \{\text{i.e. y= b + mx }\} \text{ Equation 4}$$

Chapter III
Layout of the CSTR and Design

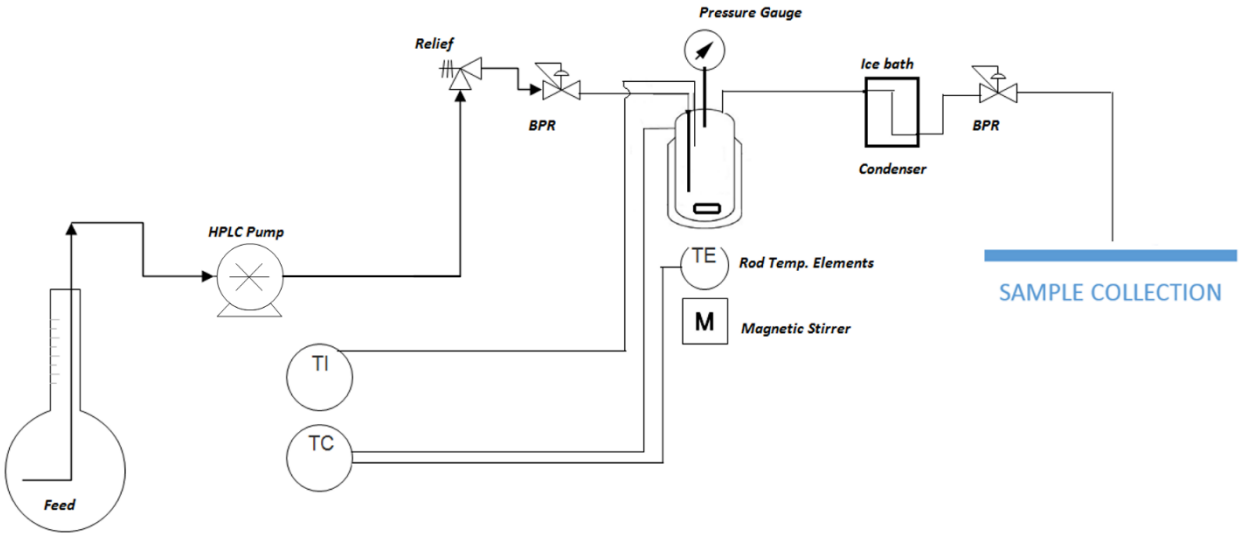

Figure 13: Layout and Experimental Setup

The setup comprised of (upstream to downstream) the feed reservoir, an HPLC pump, a relief valve rated at 1000 psi (well above operating values and below operating limits of equipment), a back pressure regulator (BPR) rated at 500 psi, the insulated CSTR, a condenser, and another 500 psi rated back pressure regulator. The pressure gauge positioned above the CSTR was used to monitor pressure during the experimental runs. The CSTR was placed between the two BPR's in the interest of maintaining reaction pressures. Two thermocouples were used to monitor temperatures, one thermocouple was located in the stainless steel shell closest to the rod heating elements of the CSTR to measure highest attainable temperatures of the system while the other thermocouple was positioned at the top of the reactor and used to measure actual reacting fluid temperatures. Two thermocouples were used in the interest of maintaining an acceptable temperature gradient without exceeding the temperature tolerance of the liner material. The temperature set point for the controller was based on the temperature readings from

the reactor shell thermocouple. A BPR malfunction could cause a spiraling effect and disrupt all readings. A blocked BPR resulting from polymerized humin formation could cause pressure buildup in the CSTR. The reduction in flow and consequent reduction of the heat sink would result in a temperature increase. This situation would imply waiting through another temperature transient. An acetone wash, sonication and pumping acetone through the BPR for 10 minutes solved flow issues by dissolving the humins blocking flow. Temperature was also found to alter the mechanical properties of the BPR. Operating at higher temperatures resulted in a pressure spike. The ice-bath condenser served to solve this problem and allow for uniformity in readings. The condenser served to stop the reaction and volatilization of reacting solution in the tubing downstream to the CSTR. The CSTR used was constructed out of stainless steel 316 owing to its mechanical properties and ease of fabrication. Despite its resistance to corrosion due to the nature of experiments to be run (low pH and high temperature) it was decided to use a lining material Polyether ether ketone (PEEK) on the inside of the working reactor so as to eliminate all contact of the reacting fluid with any metallic surface. Leaching of metal shell contaminants could be minimized by eliminating all metal contact with the fluid stream. The choice of solvent was water (discussed in previous sections). The inside pressure was to be regulated above the vapor pressure of water. All these efforts were taken to ensure homogeneous operation in the liquid phase. The insulated reactor was positioned on the magnetic pad such that the rod stirrer could attain desired mixing. The newly fabricated CSTR was seal tested using nitrogen gas at pressures above rated operating values. A feed inlet dip-tube was used to prevent back-mixing. Before beginning dehydration experiments it was necessary to make sure the mixing in the CSTR was near ideal. Several methods can be used to study and understand mixing characteristics, these will be highlighted further.

Chapter IV

Mixing

For the purpose of good mixing, several agitators were tested. The mixing characteristics were studied from tracer experiments to understand the limitations of mixing and corrective measures were employed by trying out different agitation speeds ranging from 700 rpm to 1200 rpm. When mixing tends to diverge from ideal conditions, well mixed models are inadequate. During the development of the reactor, mixing conditions were unknown. We make use of changing concentrations to understand the nature of mixing in the reactor. By using tracer experiments, either pulse inputs or step inputs, it is possible to compare data to ideal tracer curves and diagnose mixing problems. Specific tracer tests are needed to run mixing diagnostics. In all cases, the output of tracers are measured as a function of time and input concentrations.

4.1 Experimental Methods (Mixing)

For the purposes of this experiment we choose a step input for convenience. For the tracer test, we require an inert molecule which is easily detectable and inexpensive. The tracer must also possess similar properties as the reacting fluid to be tested. Inert tracers such as salt solutions are easy to work with. Also, it is inexpensive and easily detected by an in line total dissolved solids (TDS) meter. This allowed for an immediate output response to flowing feed stream.

The inline TDS meter was operated using two probes, one for measuring feed concentrations and the other for the CSTR output. Several tracer tests were performed, many of the charts comprise data that are of no consequence to the final reactor since several

modifications were applied. However we can get a good idea of what prompted some of these changes, and the identification of mixing problems.

First, different flow rates were tried out to visualize what information could be extracted from the mixing curves. The plots are concentration versus time and the curves are called "C" curves. Concentrations are normalized against the feed concentration since it is the maximum concentration attainable. We intend to see how much time it takes for the concentration of the exit stream to reach the desired "1" on the y-axis. Also, the extent of deviation between ideal and theoretical curve may be analyzed. From the data collected, it was realized that a few minutes elapsed before the output stream began to show any signs of the input tracer fluid. All readings were normalized with respect to the input concentration. For all analyses, output response was fit to the response to step input equation for CSTR

$$C_t = C_{t_0}(1 - e^{-\frac{t}{\tau}}) \qquad \text{Equation 5}$$

For the condition of 1 ml/min in Figure 14, first, the reactor was readied by setting an agitator speed of 700 rpm. The tracer input was then started and the output readings were noted in minute increments. Since the concentrations were normalized, i.e. C/C_0. The ideal curve based on Equation 6 was compared to experimental data:

$$\frac{C_t}{C_{t_0}} = 1 - e^{-\frac{t}{\tau}} \quad \text{Where t is in minutes.} \qquad \text{Equation 6}$$

Nominal residence time τ was calculated for a measured volume of 13.66ml. Nominal residence time $\tau = 13.66$ min for the first condition. (Since $\tau = \frac{Volume\ of\ reactor}{Flow\ rate}$)

For the second condition, the only change made was the flow rate. Flow was increased to 2 ml/min and the residence times changed to 6.5min. For the third condition, 3ml/min, τ=4.5 min.

For the HPLC analysis, a solution was prepared with a known amount of glucose, levulinic acid and HMF. The stock solution response area obtained from the HPLC was noted as C_0. Samples were collected after 5 minute intervals and analyzed in the HPLC. The response area was taken as C. The HPLC confirmed that the data collected using the inline TDS meter was accurate and sufficient for the mixing experiments.

4.2 Mixing Results and Discussion:

In the first mixing analysis, ideal and experimental mixing curves were plotted side by side with the intention of comparing flowrate effects. Through Figure 14 it was made clear that for a given agitation speed, flowrates impact time taken to reach maximum output concentrations. Since residence times are lowered with increased flowrates, maximum concentrations were reached sooner. Curves representing 3 ml/min flowrates attained maximum concentration around the 20 minute mark followed by the 2 ml/min which attained maximum concentrations around the 35 minute mark. Curves representing 1 ml/min could not reach maximum concentrations within 45 minutes of operation.

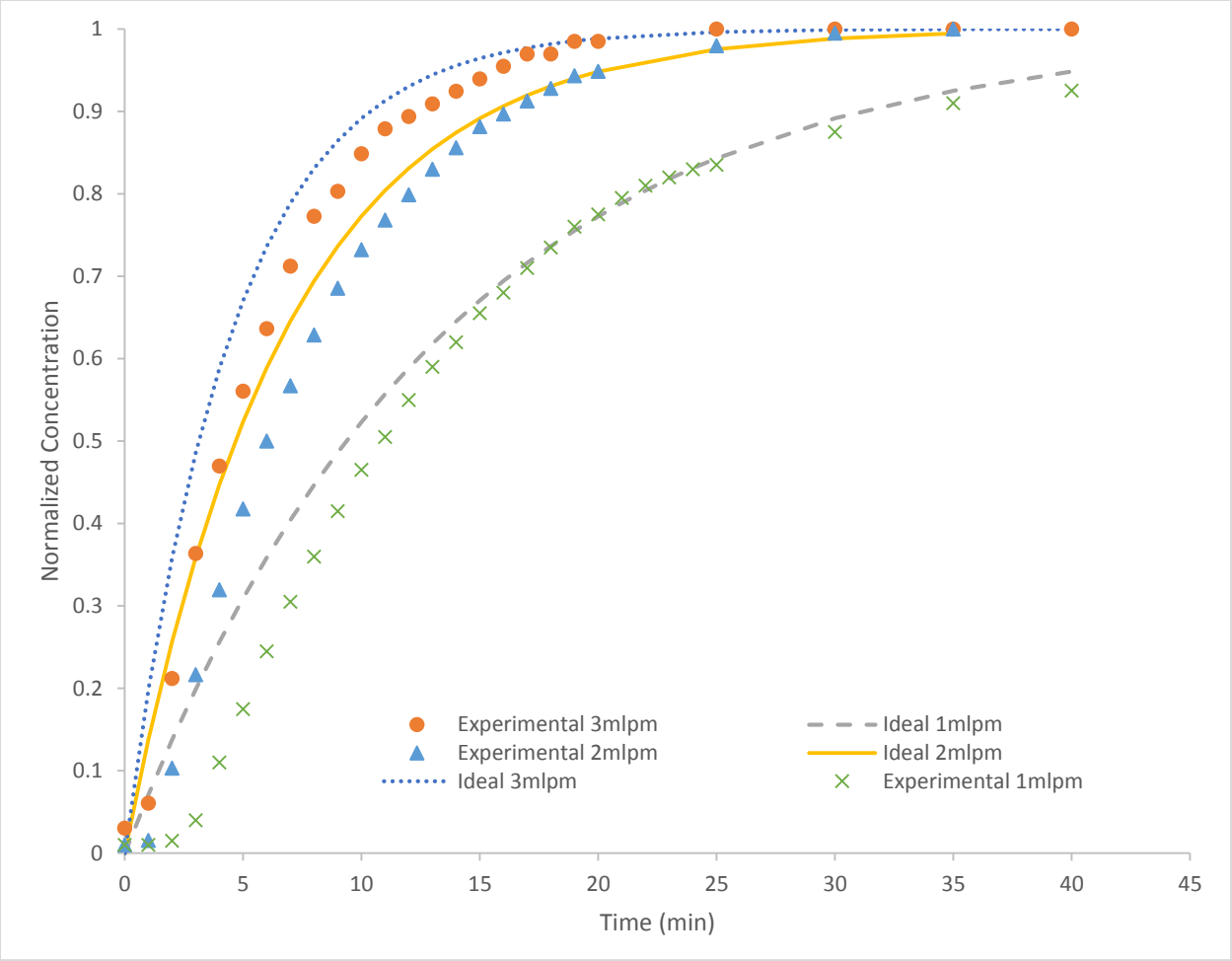

Figure 14: Mixing Curves comparing different flowrates at 700 rpm agitation.

Since preliminary analysis showed that maximum exit concentrations could be attained soonest for higher flow rates. It was decided to run the next test of a 3 ml/min flow rate keeping all other factors constant.

The bar type agitator was used in all the experiments and was observed to be unstable at higher agitation speeds. A bar type stirrer was tested between 700 and 1200 rpm. The occurrences of instability and vibration of the magnetic stirrer increased above 1000 rpm.

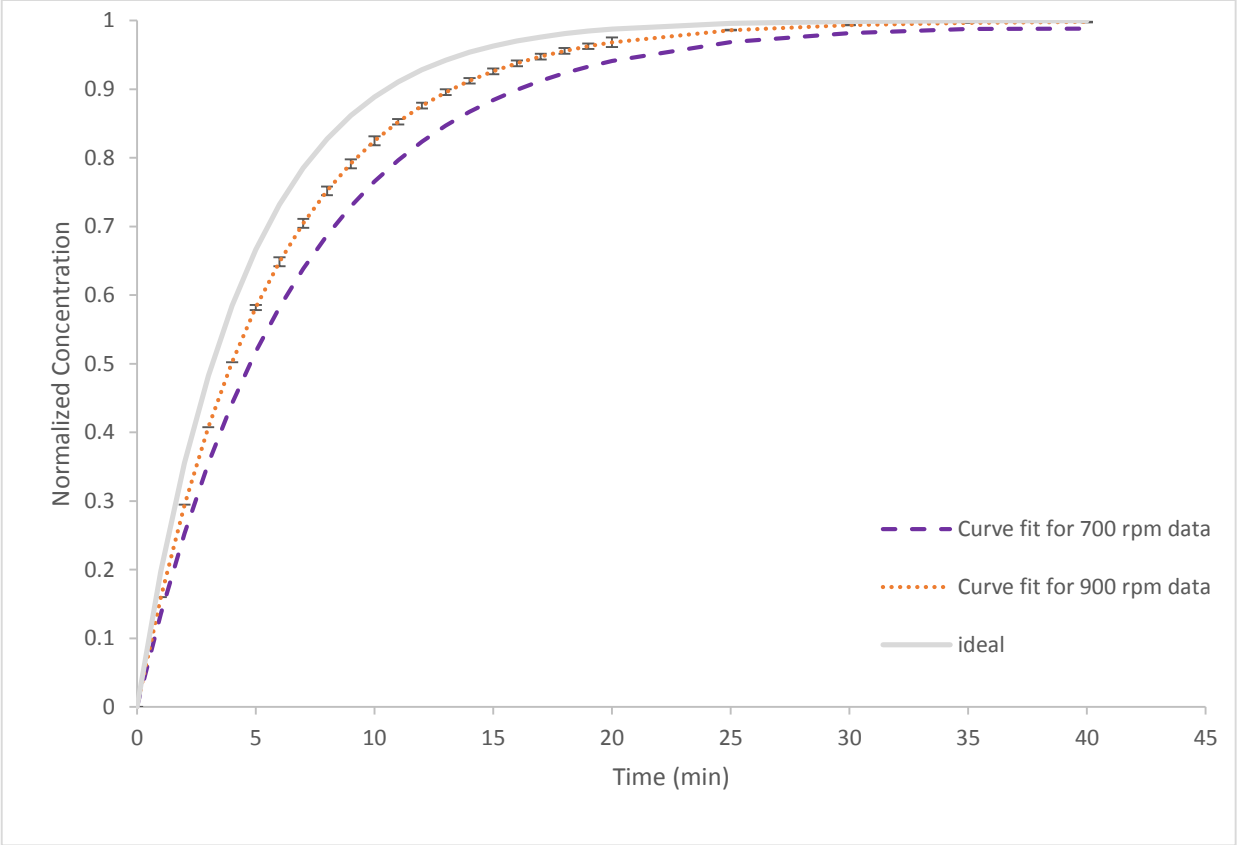

Figure 15: Effect of agitation on concentration curves. All curves above are for 3 ml/min flow rates.

In the second mixing analysis shown in Figure 15, effect of agitation speeds was studied. The flow rate was kept constant at 3 ml/min and two tracer tests were performed, one at 700 rpm and the other at 900 rpm using the same feed solution. Ideal curves were fit to the experimental data. The influence of simply changing agitation is illustrated in Figure 15. There was a qualitative increase in mixing without any instability at 900 rpm agitation speeds. The final output concentrations obtained for the 700 rpm experiment were lower than final output concentrations seen in the 900 rpm agitation experiments within the 40 minute mark. This comparison confirmed increased mixing efficiency for higher agitation speeds.

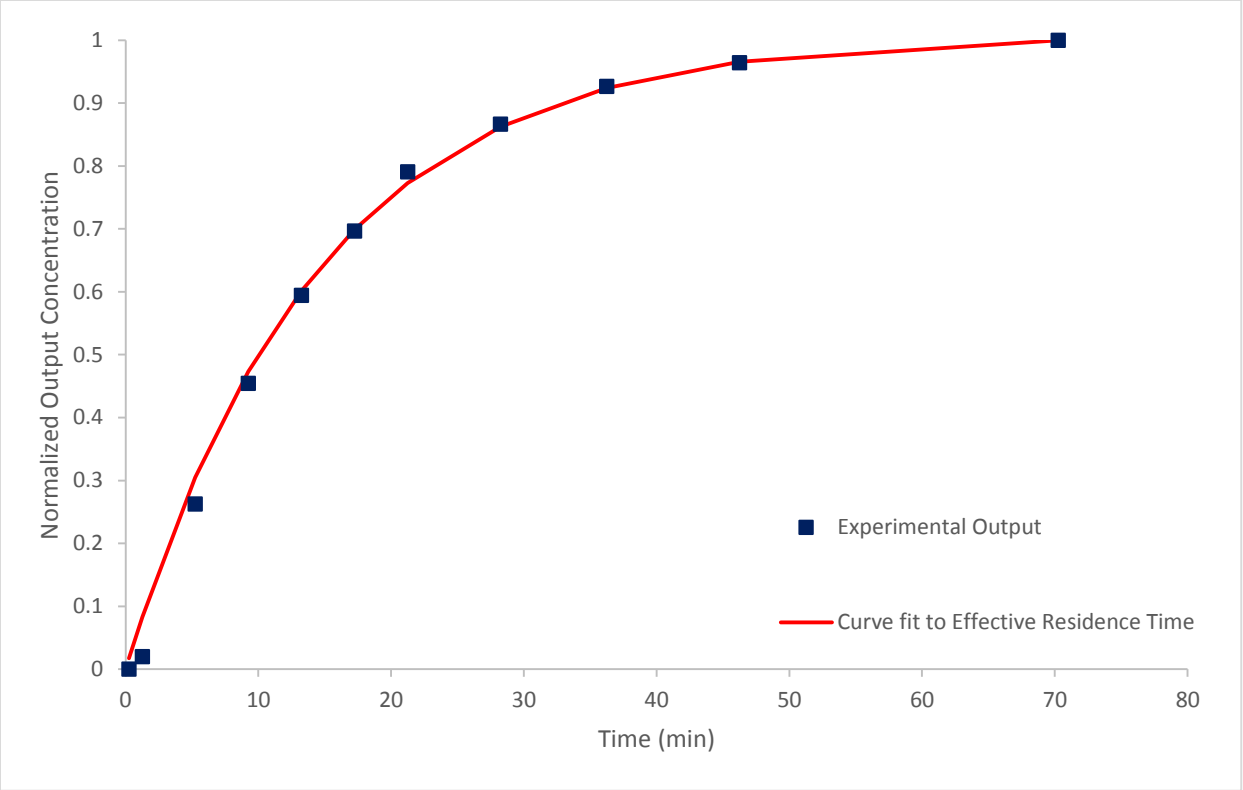

Figure 16: Calculation of effective residence time from tracer data. Experimental data collected at 900 rpm agitation and 1ml/min flow rate.

Nominal residence times would be insufficient to accurately calculate rates owing to possible dead volume. The measured volume of the CSTR was 13.66 ml. Experimental data collected for the final curve are shown in Figure 16. The curve used to fit the experimental data represents a residence time of 14.60 min. This is our effective residence time for a flow rate of 1 ml/min and agitation of 900 rpm. A larger effective residence time calculated would normally indicate that the measured volume of the reactor failed to account for the dead volume relative to flow rate. In the case of our experimental setup, pump flowrates were found to deviate from 1 ml/min. This could explain higher effective residence times as confirmed in Figure 16.

Although higher flow-rates were desirable for reaching maximum concentrations sooner, 1ml/min was chosen as the set operating volumetric flow-rate. Larger flow rates would translate

to a larger heat sink. Maintaining high temperatures with higher flow rates could result in large thermal gradients sometimes exceeding the operating temperature specifications of the liner material.

Chapter V

Dehydration Experiments

5.1 Analytical Equipment and Chemicals

All dehydrations were carried out in the CSTR setup described above using sulfuric acid as the catalyst. The chemicals obtained from all sources were used as is without any additional purification. Alpha-D-(+)-glucose, 99+% and sulfuric acid 95% were purchased from ACROS Organics, D-Fructose lab grade from Fischer Scientific, D-(+)-xylose used in experiments was sourced from Sigma Aldrich. K type thermocouples (OMEGA) were used for the temperature measurements. Cartridge heaters were used to heat the reactor system. Analysis was carried out in an HPLC (Hi-Plex H+ column Agilent Technologies) using the sugars PLEX column. Sugars were analyzed using the refractive index peaks and dehydration products were measured using ultra violet (210 nm) peaks. A sulfuric acid solution with a pH of 2 was used as the mobile phase.

5.2 Selection of Reactor

A preliminary study was conducted to understand the nature of reaction and chemistry, industrial applications, text book methods and formulae. Several types of reactors may be used for a dehydration reaction. Some research is focused on batch reactors for dehydrations in a biphasic setting. The Biofine process (an industrial scale setup for production of HMF, levulinic Acid and furfural) combines hydrolysis and dehydration in a plug reactor and a CSTR. The choice of reactor type is based on specific goals of the study, economy, practicality and basic functioning. Our need was based on running liquid phase reactions. The decision of using a

CSTR over other reactor types was based on several factors. A CSTR can be used for uniform products and continuous production. The temperature could be controlled and distributed uniformly due to the well mixed nature of a CSTR. Near isothermal conditions were needed in the CSTR to be able to precisely maintain and report reaction temperatures. Many aspects of the CSTR were planned, designed and controlled to make this possible. Calculations used to determine rate constants and other parameters in the proceeding part of the text rely on accurate recorded measurements of temperature. Specific rate data could be collected at several points for a given set of conditions, thereby increasing the accuracy of data. Mixing transients could be well documented through tracer tests and accurate steady state data could be collected for a given reaction. Data acquired at steady state was a crucial factor in the kinetic study. Steady states were important because data for rate constants needed to be calculated for a fixed temperature (temperature steady state). Steady state in concentrations also needed to be maintained to understand the influence of specific concentrations of protons and sugars in feed.

We choose homogeneous liquid phase reactions due to the added advantages. There are no transport limitations experienced as are with heterogeneous catalysts. Surface anomalies do not need to be considered. Other concerns that need to be addressed when using solid catalysts are catalyst site characterization, poisoning and deactivation. The choice of acid was based on ease of measurement of acid strength. Sulfuric acid has been studied extensively for use in dehydration experiments (HMF and furfural production) and its selection as a catalyst would simplify most experimental techniques [37, 64].

5.3 Experimental Procedure

The decision of running the reactor over a range of reactor temperatures (130-150℃) was based on the literature study and temperature limitations of the CSTR. Carefully prepared feed solutions at ambient temperatures were checked using a calibrated pH probe (buffers pH values were 4.01 and 7.01) to ensure that proton concentrations matched calculations based on measured acid loading. Although acid loading was measured in molar units, an equivalent proton concentration based on dissociation was developed and used. A feed solution sample was analyzed against the calibrated HPLC chromatogram data to confirm that the sugar loadings were within boundaries. The pump was set to 1ml/min. De-ionized water was pumped through the reactor while the temperature reached the set point. Feed solution was pumped through the CSTR only after all temperature transients were overcome. End of loading feed solution was taken as t = 0. The mixing-flow transient for this residence time amounts to approximately 68 minutes Figure 17.

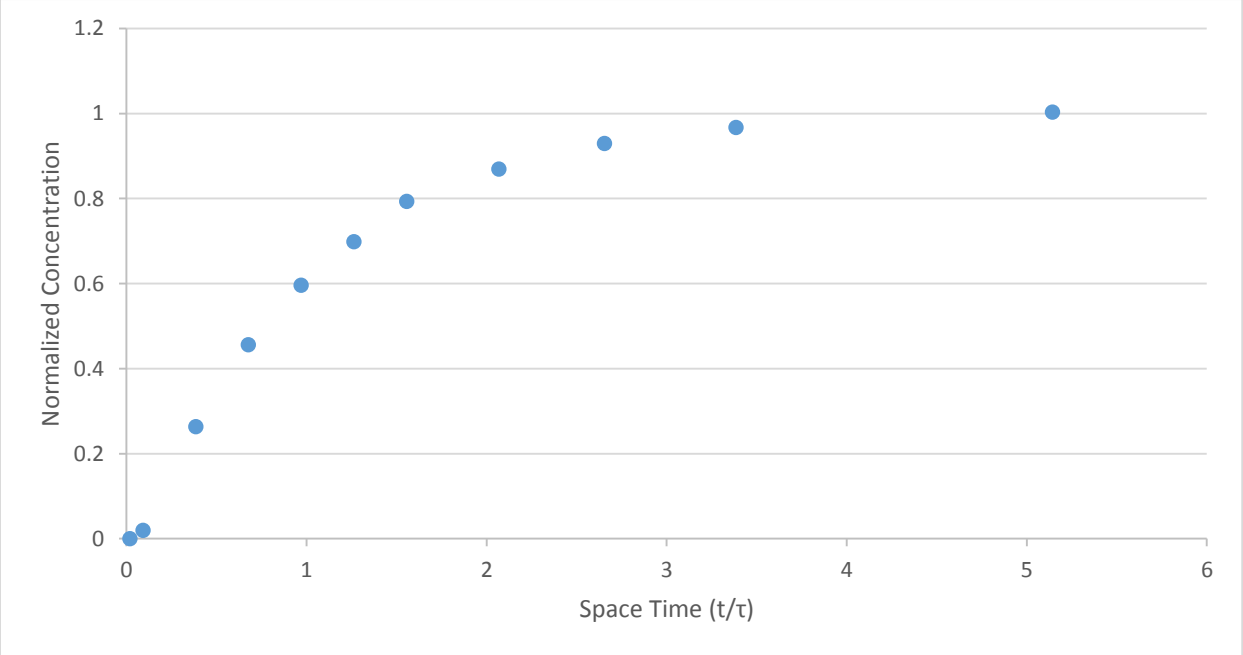

Figure 17: Visualization of space time for steady state. Approximately 5 space times needed for steady state.

A total of 5 residence times are needed to ensure steady state with regard to flow. Once steady state was achieved, 4 samples were collected for every experiment to ensure uniformity. The first sample was collected at t = 80 min. A single sample was collected every 3 minutes to be able to ensure uniformity and reproducibility in data.

5.4 Analytical Methods

Densities of output solutions after experiment were compared to feed solutions before experiment. The change in density after completion of experiment were negligible. However, due to temperature dependence of densities during reaction, feed densities needed to be measured and recorded. Feed densities were measured manually by weighing out 100 ml of the unused feed solution. Concentrations of the feed input of an experiment and also output concentrations were measured from calibrated HPLC chromatogram areas. Concentration data was recorded in moles per sample volume. Carbon moles were calculated for both input and output. One mole of a hexose sugar corresponds to 6 moles of carbon. Similarly one mole of a pentose corresponds to 5 moles of carbon. Carbon moles were calculated for all inputs and corresponding outputs. The difference in measured inputs and outputs helped maintain a carbon balance. The carbon balance was maintained within a range of 5% error. Large deviations in the carbon balance would be indicative of a system leak or unaccounted reactant or product. Conversions were calculated based on the amount of product produced per unit reactant (sugar) fed to the reactor i.e. moles product per mole reactant fed. Rates of reaction were calculated based on the product.

$$r = \frac{\text{moles produced per volume}}{\text{residence time}} \qquad \text{Equation 7}$$

Rate estimations are affected by changing densities. As temperature increases, fluid in the reactor expands and its volume increases. This causes a perturbation in residence time relative to that measured at room temperature. Since residence times are used to estimate rates of reaction (Equation 7), it is important to correct for temperature-dependent changes in density under reaction conditions. The volume increase is a function of initial density and depends on Volumetric Expansion Coefficient (β) with units /℃ and Bulk Modulus (E) with units N/m^2. The combined effect of heat and pressure can be calculated as:

$$\varrho = \frac{\varrho_0}{(1 + \beta\,(t_1 - t_0))\times(1 - (p_1 - p_0)/E)} \qquad \text{Equation 8}$$

ϱ: Density at operating temperature

ϱ_0: Density of feed at room temperature

β: Volumetric expansion coefficient taken as 0.0002 (m^3/m^3 ℃) (water)

$t_1 - t_0$: Difference in final temperature and room temperature (℃)

$p_1 - p_0$: Difference between ambient pressure and reactor pressure at operating temperature (Pa) fixed for all reactions at 33.5×10^5 Pa

E: Bulk Modulus taken as 2.2×10^9 N/m^2

Proton concentrations of reacting solutions were calculated by solving equilibrium equations.

$$H_2SO_4 \leftrightarrow H^+ + HSO_4^- \qquad \text{Equation 9}$$

$$HSO_4^- \leftrightarrow H^+ + SO_4^- \qquad \text{Equation 10}$$

$$H_2O \leftrightarrow H^+ + OH^- \qquad \text{Equation11}$$

$$k_{a1} = \frac{[H^+][HSO_4^-]}{[H_2SO_4]}$$ Equation 12

$$k_{a2} = \frac{[H^+][SO_4^-]}{[HSO_4^-]}$$ Equation 13

$$k_w = \frac{[H^+][OH^-]}{[H_2O]}$$ Equation 14

Calculation of dissociation constant of water k_w is as under

$\ln(k_w) = 2.70291 - 2.6105 \times 10^3 T$ (Temperature T in degree Celsius) Equation 15

Sulfuric acid is a diprotic acid, i.e. It contains two protons. Sulfuric acid may dissociate to donate one proton or it may donate the second proton as well. The first dissociation is a strong acid dissociation. The dissociation constant k_{a1} for the first dissociation is large of the order of 2.4×10^6. We may assume complete dissociation of the first proton due to the high value of $k_{a1.}$ Dissociation of sulfuric acid in water is exothermic. We know that the proton concentration of the solution will decrease with an increase in temperature. We need to quantify this decreased proton concentration by solving equilibrium reactions and considering all of the temperature dependent terms. The second dissociation constant k_{a2} (temperature dependent) is a weak acid dissociation and is known for the range of operating conditions. It may be calculated using the Debye-Huckle equations for ionic strength.

$\log K_2 = 56.889 - 19.8858\ log\ T - \frac{2307.9}{T} - 0.006473T\ (Temperatures\ T\ in\ Kelvin)$

Equation 15

5.5 Kinetic Results and Discussion

5.5.1 Glucose

Before rate data were collected, corrections were applied to account for the change in density and the change in proton concentration of reacting solution. The effect of temperature on density was studied and illustrated in Table 1 by evaluating the percentage change in density for the highest and lowest temperatures within operating temperature range. Residence times were affected as a result of this change in effective volumetric flow-rate. Rates were found to vary by up to 4.27% for higher temperatures as can be seen in Table 2. Change in densities of reacting solutions after exiting the CSTR were negligible and not considered owing to small conversions.

TABLE 1: EFFECT OF TEMPERATURE ON DENSITY.

Operating Temperature ℃	Initial density at 25℃ (kg/l)	Final density at operating temp (kg/l)	% Change
150	1040	1016	2.3
	1014	990	2.3
	1004	981	2.3
	1001	978	2.3
120	1040	1022	1.7
	1014	996	1.7
	1004	986	1.7
	1001	983	1.7

TABLE 2: MAXIMUM DIFFERENCE IN RATES CALCULATED BY ACCOUNTING FOR CHANGE IN EFFECTIVE RESIDENCE TIME.

Temp ℃	Glucose wt %	pH measured with probe	Rate HMF (mol/l.min)	Volumetric flow rate (ml/min)	Residence time at 25℃	Rate not accounting for temp.	Density at 141℃	Effective flow-rate	Residence time at 141℃	Rate at 141℃	Difference in calculated rates
141	1	2.01	1.678E-07	0.959	14.23	1.609E-07	979.79	0.979	13.64	1.7E-07	4.27%

Most mechanistic studies neglect the effect of proton concentrations. They instead rely on rate measurements for specific pH values [52.] The activation energies and pre-exponential factors calculated in these studies lump the effects of proton concentrations. This is possible through the use of the modified Saeman equation which is similar to the Arrhenius equation. This equation can be expressed as;

$$k = A_0.[H]^m e^{\frac{-E_a}{RT}} \qquad \text{Equation 16}$$

Where, A_0 is the Saeman pre-exponential factor, H is the proton concentration and m indicates temperature dependence of H.

In this project, we focus on calculating proton concentrations at reaction temperatures through the use of measured proton concentrations at room temperature. Dissociation is temperature dependent and changes for every temperature. Molar concentrations of protons could not be measured during the reaction and therefore called for calculated values. The inclusion of proton concentrations at reaction temperature are needed for calculation of rate constants. Our plot of the Arrhenius equation in Figure 20 includes the effect of proton concentrations separately and does not require normalizing the pre-exponential factor with proton concentrations. We avoid the use of lumped pre-exponential factors and hence are able to express partial orders in both sugars and protons.

Table 3 illustrates recorded values of pH and H+ at room temperature with corresponding pH and H+ values at reaction temperatures. The temperature column represents experimental reaction temperatures. The difference in the proton concentrations at room temperature and at reaction temperatures may be represented as a percentage as shown in the last column of Table 3.

Largest changes in proton concentration could be observed for higher temperatures and higher pH values. Proton concentrations were found to vary with temperature by up to 45.9% for higher temperatures of 141℃ and pH 2.

TABLE 3: EFFECT OF TEMPERATURE ON PROTON CONCENTRATION.

Temperature ℃	pH @25 ℃	H+ @ 25℃ (mol/l)	pH @ Final Temperature	H+ @ Final Temperature (mol/l)	% difference in H+ due to heating
123.00	1.00	0.099	1.037	0.091	8.57
131.80	1.50	0.031	1.592	0.025	22.36
132.00	2.00	0.008	2.234	0.005	43.45
132.50	1.00	0.099	1.038	0.091	8.77
141.00	2.01	0.008	2.241	0.005	45.90
141.00	1.50	0.031	1.594	0.025	22.95
141.00	1.00	0.099	1.038	0.091	8.92
103.60	2.00	0.008	2.201	0.006	33.05
122.00	2.00	0.008	2.226	0.005	40.59
123.00	2.07	0.008	2.243	0.005	40.93
123.00	1.50	0.031	1.590	0.025	21.65

Rates of dehydration of glucose were calculated based on moles of HMF produced per unit volume per unit time. The corrected residence times contributed to reliable rate measurements illustrated in Table.4.

TABLE 4: HMF FORMATION RATES FROM GLUCOSE FEED SOLUTION. (HMF YIELDS RANGING FROM 0.26 MMOL/L FOR PH 2, 1 WT % GLUCOSE TO 226.02 MMOL/L FOR PH 1, 10 WT % GLUCOSE)

123℃			132℃			141℃		
Glucose (wt %)	pH	Rate (mol/l.min)	Glucose (wt %)	pH	Rate (mol/l.min)	Glucose (wt %)	pH	Rate (mol/l.min)
1	2	1.87E-08	1	2	5.83E-08	1	2	1.67E-07
	1.5	6.29E-08		1.5	1.88E-07		1.5	5.52E-07
	1	2.28E-07		1	7.98E-07		1	1.77E-06
2	2	3.76E-08	2	2	1.21E-07	2	2	3.46E-07
	1.5	1.25E-07		1.5	3.89E-07		1.5	1.12E-06
	1	4.80E-07		1	1.44E-06		1	3.42E-06
5	2	9.42E-08	5	2	2.81E-07	5	2	8.39E-07
	1.5	2.95E-07		1.5	9.52E-07		1.5	2.62E-06
	1	1.22E-06		1	3.62E-06		1	8.38E-06
10	2	2.05E-07	10	2	5.64E-07	10 `	2	1.61E-06
	1.5	5.36E-07		1.5	1.77E-06		1.5	4.82E-06
	1	2.04E-06		1	6.69E-06		1	1.53E-05

Rate data were collected at constant temperature. From the rate law, we have;

$$r = kC_g^a C_{H+}^b \qquad \text{Equation 17}$$

Rate data were calculated at several known concentrations of sugar and protons. We are able to extract information from the specific groups of data points. By grouping the rates measured at fixed pH (proton concentrations) and fixed sugar concentrations it is possible to determine partial orders using kinetic analysis.

Rate data collected for a constant pH by varying sugar concentrations helps express the effect of sugar concentrations at that temperature. In the case of this experiment, proton concentrations are fairly unchanged during reaction since protons play the role of a catalyst. For constant pH, the rate law may be represented as;

$$lnr = lnk' + alnC_g \qquad \text{Equation 18}$$

Lumped rate constant k' as illustrated in Table 5 may be obtained from the regression plot of multiple data points.

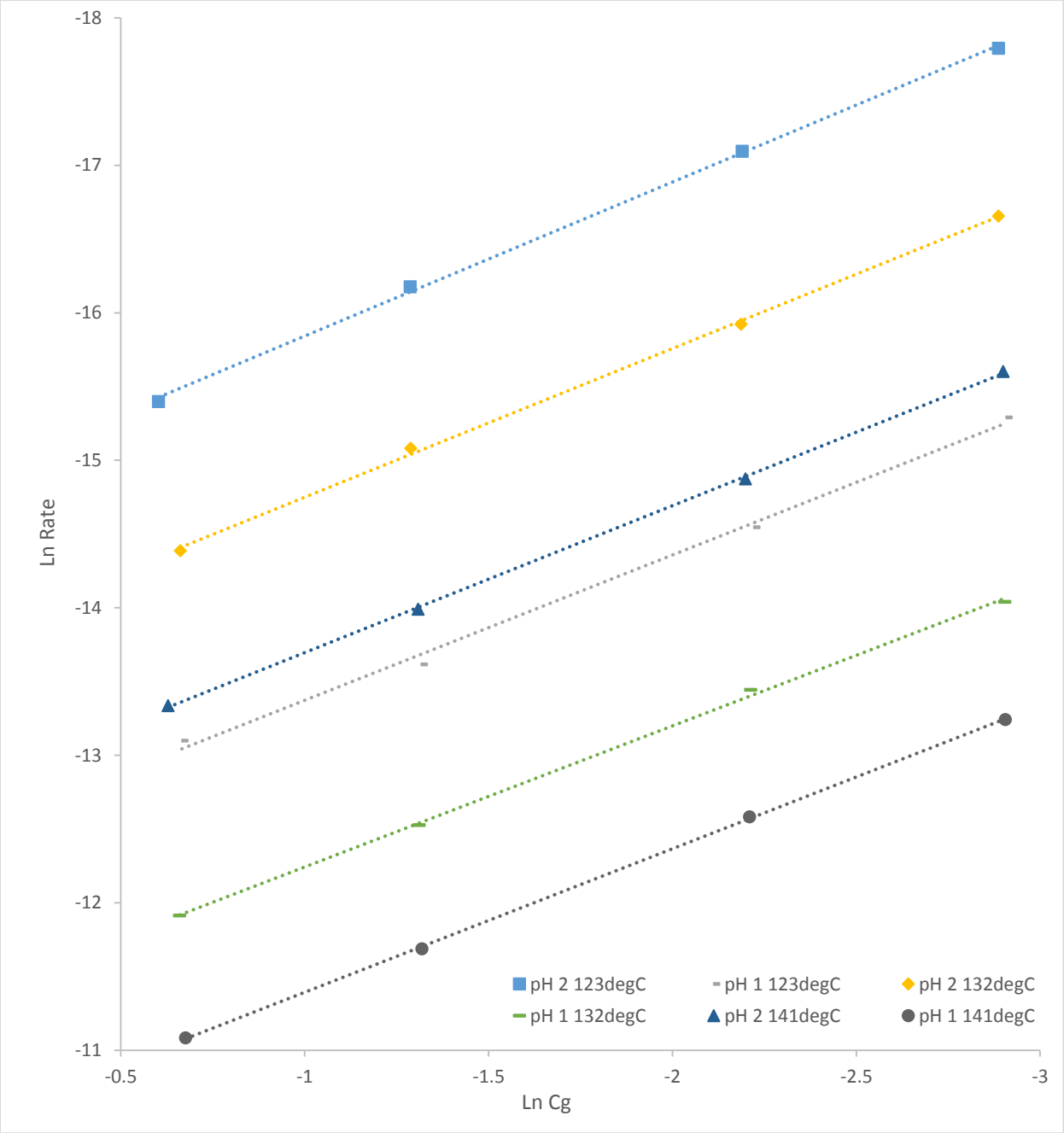

Figure 18: ln Rate vs ln Cg for constant pH

TABLE 5: LUMPED RATE CONSTANTS FOR GLUCOSE EXPERIMENTS (CONSTANT H+ CONC.)

pH	Lumped Rate Constant k' (1/min)	Temperature ℃
2	3.41E-07	123
1.5	1.08E-06	
1	4.55E-06	
2	1.02E-06	132
1.5	3.51E-06	
1	1.35E-05	
2	3.11E-06	141
1.5	9.75E-06	
1	3.14E-05	

TABLE 6: REACTION ORDERS FOR CONSTANT PH DATA (GLUCOSE EXPERIMENTS)

Temperature ℃	pH	Reaction Order
123	1.0	0.945
	1.5	1.008
	2.0	1.044
132	1.0	0.986
	1.5	0.990
	2.0	0.997
141	1.0	0.973
	1.5	0.957
	2.0	0.963

Data in Figure 18 allows us to observe the cumulative set of experimental points for constant pH. Each line in the graph represents four reactions carried out at a single pH and fixed temperature by varying glucose concentration alone. It can be determined from Table 6 that partial order is approximately “1” with respect to glucose.

A similar analysis for constant glucose loading may be performed. For constant glucose concentrations, the rate law may be represented as;

$$\ln r = lnk'' + b\ln C_{H+} \qquad \text{Equation 19}$$

Here, k" illustrated in Table 7 are the lumped rate constants.

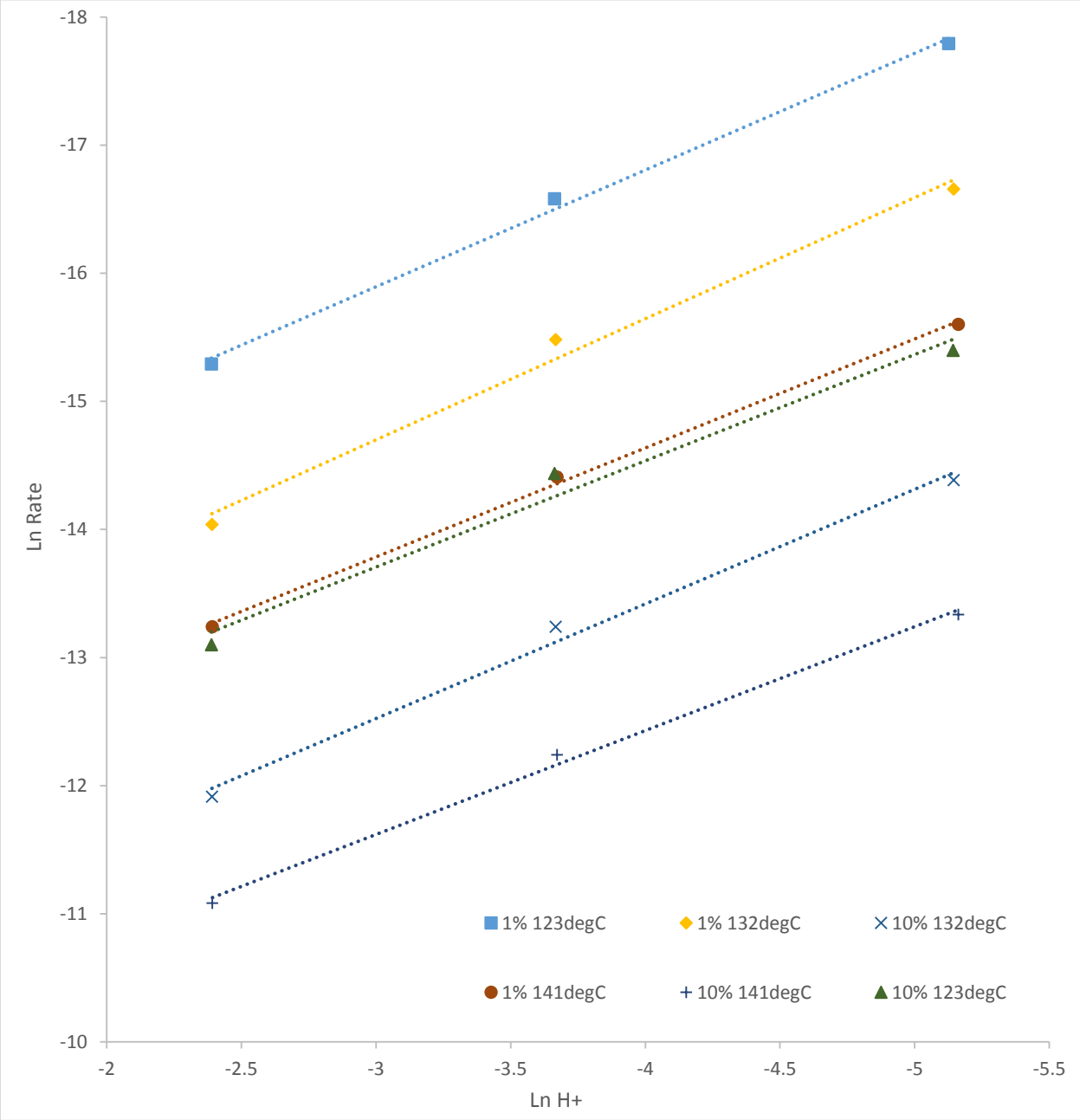

Figure 19: ln Rate vs ln H+ for constant Glucose loading

TABLE 7: LUMPED RATE CONSTANT K" FOR CONSTANT GLUCOSE LOADING

Temperature ℃	Glucose (g/l)	Lumped Rate Constant k" (1/min)
123	10	2.45E-06
	20	4.90E-06
	50	1.15E-05
	100	2.09E-05
132	10	7.39E-06
	20	1.53E-05
	50	3.73E-05
	100	6.95E-05
141	10	2.17E-05
	20	4.43E-05
	50	0.000103
	100	0.00019

Data in Figure 19 allows us to observe the cumulative set of experimental points for constant glucose concentration. Each trend line represents data collected at a fixed temperature and glucose concentration for three different pH values. It can be determined that partial order is approximately one with respect to protons.

First order reactions (partial) in glucose and protons individually are observed in the preceding sections. Once we have our partial orders, overall order of the reaction may be calculated as

$$n = a + b \qquad \text{Equation 20}$$

From our data it is clear that overall order of reaction is "2". Since units of k are

$$min^{-1}\left(\frac{mol}{l}\right)^{[1-(a+b)]} \qquad \text{Equation 21}$$

We get units of the overall rate constant as l/(mol.min). We may now use the rate law with known orders to ascertain the overall rate constant k at each temperature.

TABLE 8: SECOND ORDER RATE CONSTANTS FOR GLUCOSE CALCULATED FROM EXPERIMENTAL RATES

Temperature ℃	Rate constant [l/mol.min]
123	4.38E-05
132	0.0001
141	0.0003

Rates measured for all concentrations of glucose and protons are used in all proceeding analyses. Rate constants were calculated for second order reaction in protons and sugar at every reaction temperature. The least squares numerical method was used to calculate k.

Calculation of Rate Constant, Activation Energy and Pre-Exponential factor.

The Arrhenius plot or Ln k versus (1/T) graph was used to explore the temperature dependence of the dehydration reaction.

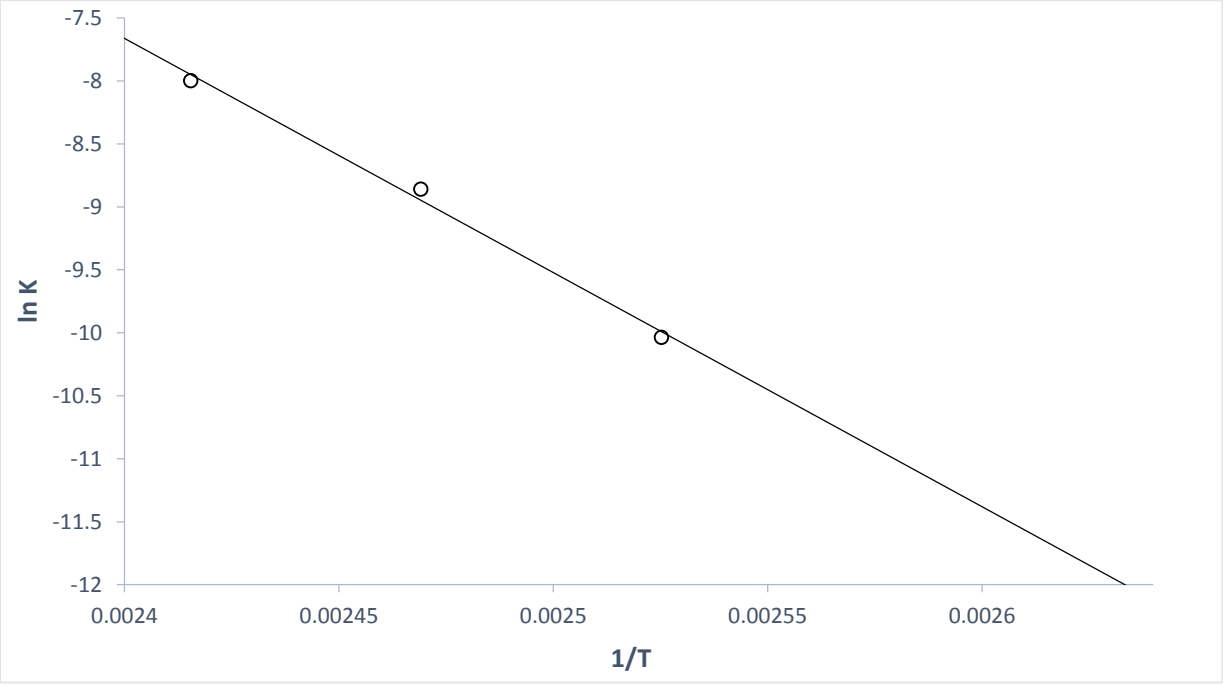

Figure 20: Arrhenius plot (Glucose)

The slope of this plot corresponds to Ea/R (shown in literature survey). Ea is calculated as 154.5 ± 11.75 kJ/mol. Activation energy value from literature studies found to be 118±37.5 kJ/mol.[49] Pre-exponential factor A corresponds to the exponent of the intercept. A is calculated as 1.115E+16 l/(mol.min).

Similar experiments and analyses were carried out with fructose and xylose.

5.5.2 Fructose

Fructose dehydration rates as experimentally determined are illustrated in Table 8. Fructose dehydration is found to have higher rates than glucose dehydration and are in agreement with literature. Rate constants were used to compare rates of dehydration of glucose and fructose and are presented in Table 10. Rates of fructose dehydration were found to be 99% faster than glucose dehydration. This is in accordance with the cyclic intermediate scheme presented in our study of mechanism. The alternative theory of reactions proceeding via open chain intermediates is unable to explain a difference in rates of glucose and fructose dehydrations. The elimination of the 3-hydroxyl group to form the enol that is thought to take place through the liner chain mechanism should commence at the same rate for both glucose as well as fructose. However, this is not the case. Both dehydration reaction schemes lead to the formation of HMF through the fructofuranosyl intermediate. Cyclic/Ring mechanisms leading to the intermediate formation through β-elimination can explain differential rates between glucose and fructose. Anomeric equilibria and the effects of temperature on tautomerism were not explored in this study.

TABLE 9: HMF FORMATION RATES FROM FRUCTOSE FEED SOLUTION (EXPERIMENTAL).

Temp ℃	pH	Fructose (mol/l)	Rate (mol/l.min)
103.6	2	0.055	1.91E-07
		0.110	4.52E-07
		0.274	1.13E-06
112.5	1	0.053	1.19E-05
		0.257	5.78E-05
122.4	1	0.049	3.01E-05
		0.241	0.0001
104.1	0.5	0.052	1.64E-05
		0.251	8.03E-05

Fructose rates were measured for a number of conditions. The constant pH data are plotted as under.

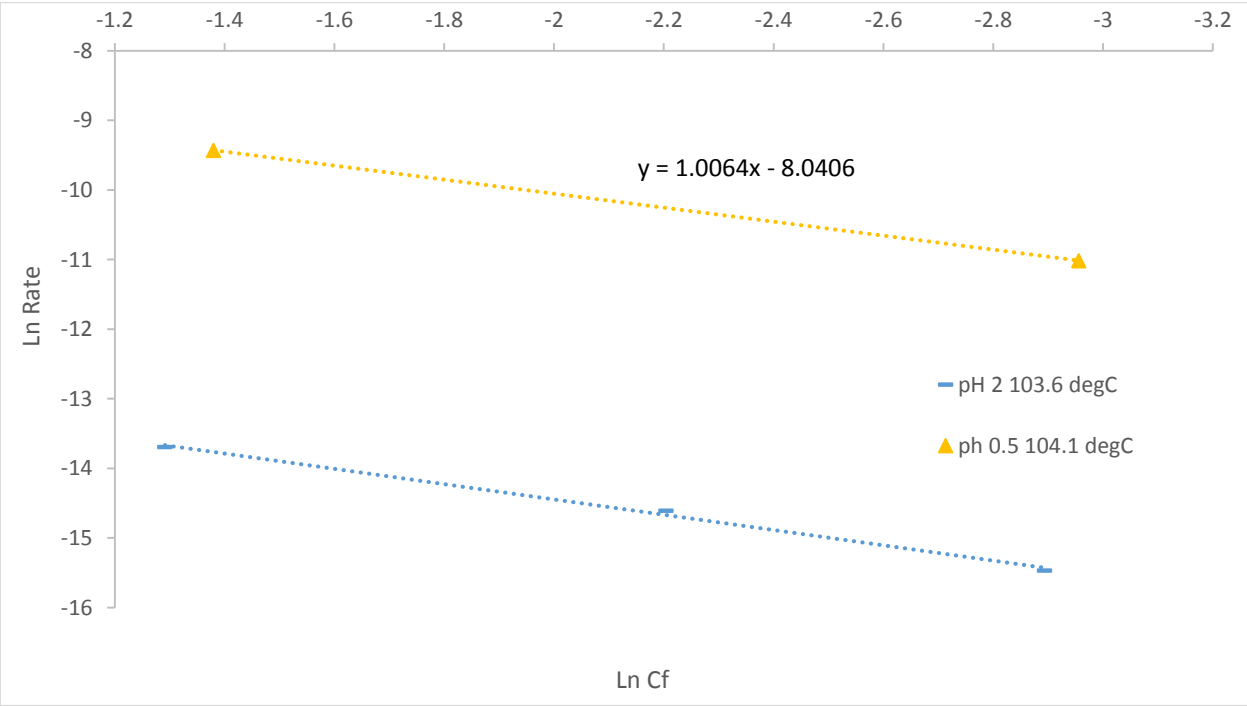

Figure 21: ln Rate vs ln Cf

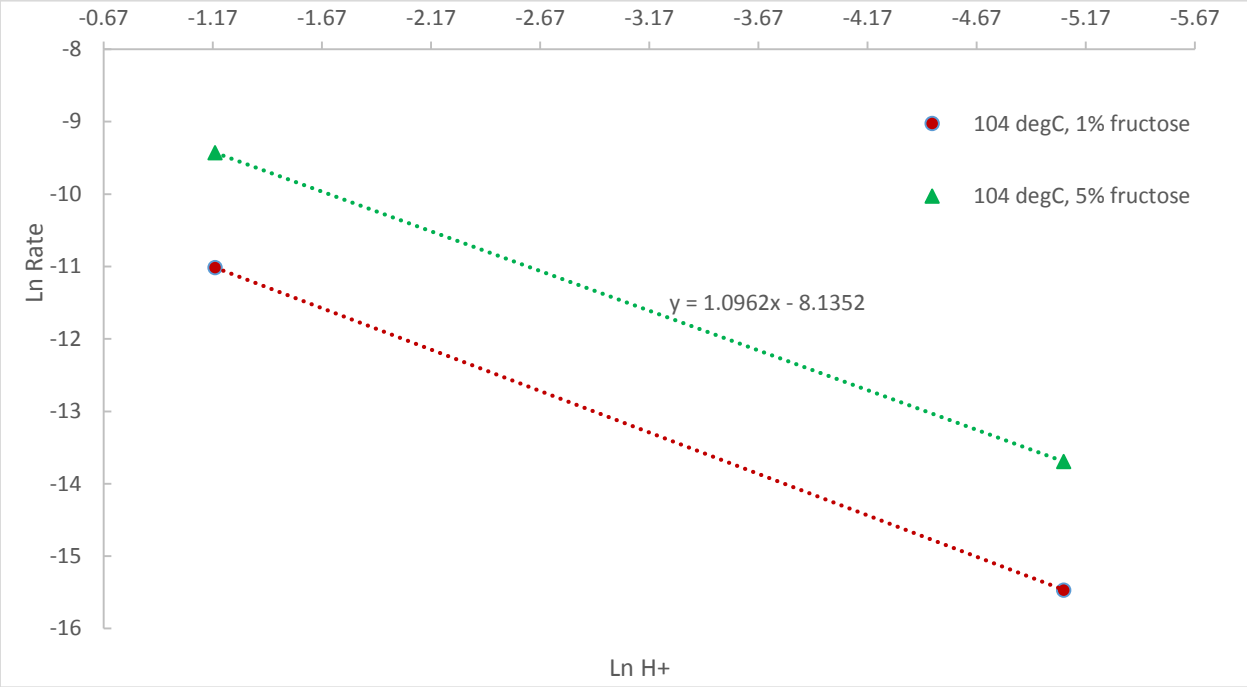

Figure 22: ln Rate vs ln H+ (Fructose)

Figure 21 and Figure 22 establish that fructose dehydration rates are first order in both protons and fructose. Since orders have been established, we may proceed to calculate rate constants and consequently barriers and other kinetic constants for fructose dehydration.

TABLE 10: SECOND ORDER RATE CONSTANTS FOR FRUCTOSE CALCULATED FROM EXPERIMENTAL DATA.

Temperature ℃	Rate constant [l/mol.min]
103.6	0.0006
112.5	0.002
122.4	0.006
104.1	0.001

The Arrhenius plot better represents temperature effects on rate. The Arrhenius plot for fructose shown in Figure 23.

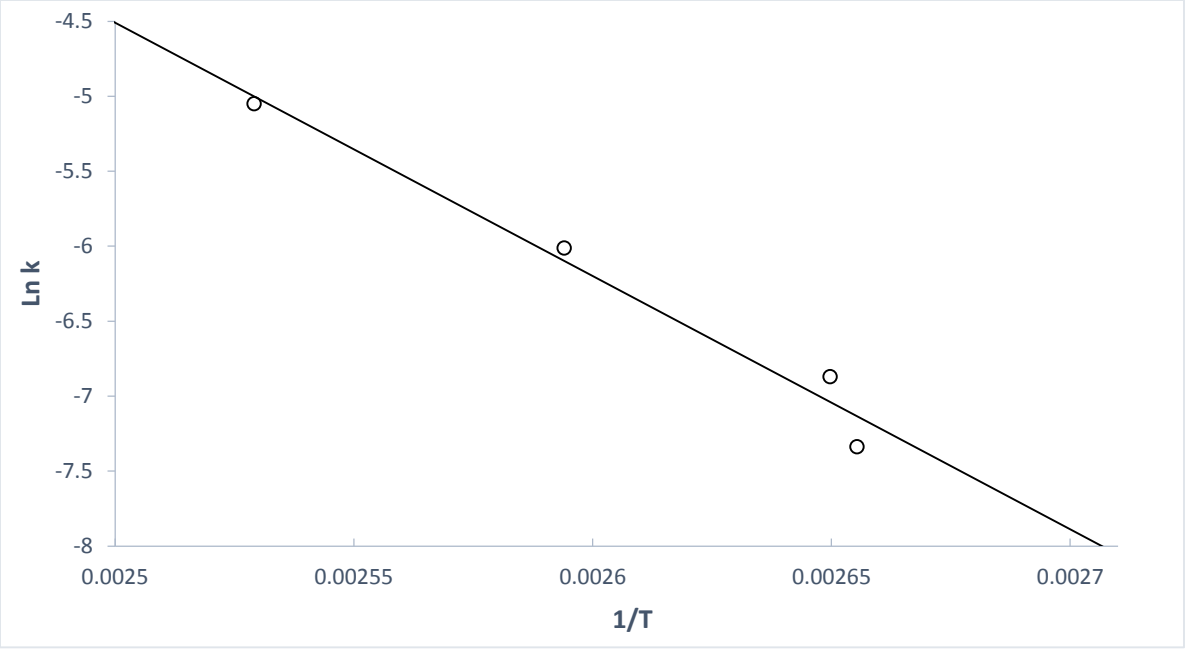

Figure 23: Arrhenius plot (Fructose)

The activation energy obtained from this data is 140.45 ± 16.306 kJ/mol. Literature data for fructose dehydrations with sulfuric acid indicate an Ea of approximately 136 kJ/mol.

5.5.3 Xylose

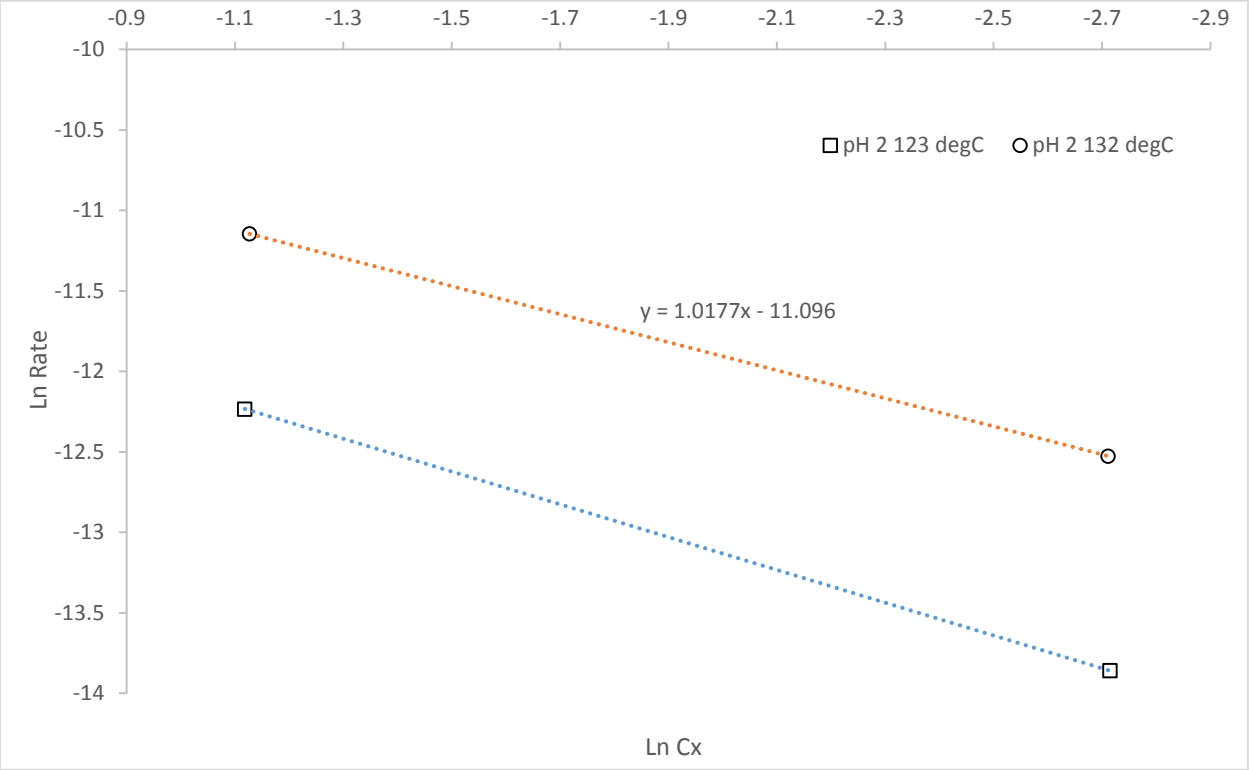

Figure 24: ln Rate vs Ln Cx

Xylose data were collected for only one pH value and two temperatures. The rate increase facilitated by an increase in temperature from 123 to 132 ℃ is clear in Figure 24. Both sets of data were obtained for a pH of 2. Xylose dehydration is also found to be first order in sugar and protons. Xylose rates used in the analysis are shown in Table 9.

TABLE 11: RATES OF FURFURAL FORMATION FROM XYLOSE FEED SOLUTION.

Temperature ℃	Xylose (wt %)	pH	Rate (mol/l.min)
123	1	2	9.577E-07
	5	2	4.863E-06
132	1	2	3.632E-06
	5	2	1.444E-05

TABLE 12: SECOND ORDER RATE CONSTANTS FOR XYLOSE CALCULATED FROM EXPERIMENTAL RATE DATA

Temperature ℃	Rate constant [l/mol.min]
123	2.48E-05
132	6.87E-05

The Arrhenius plot for xylose is shown in Figure 24.

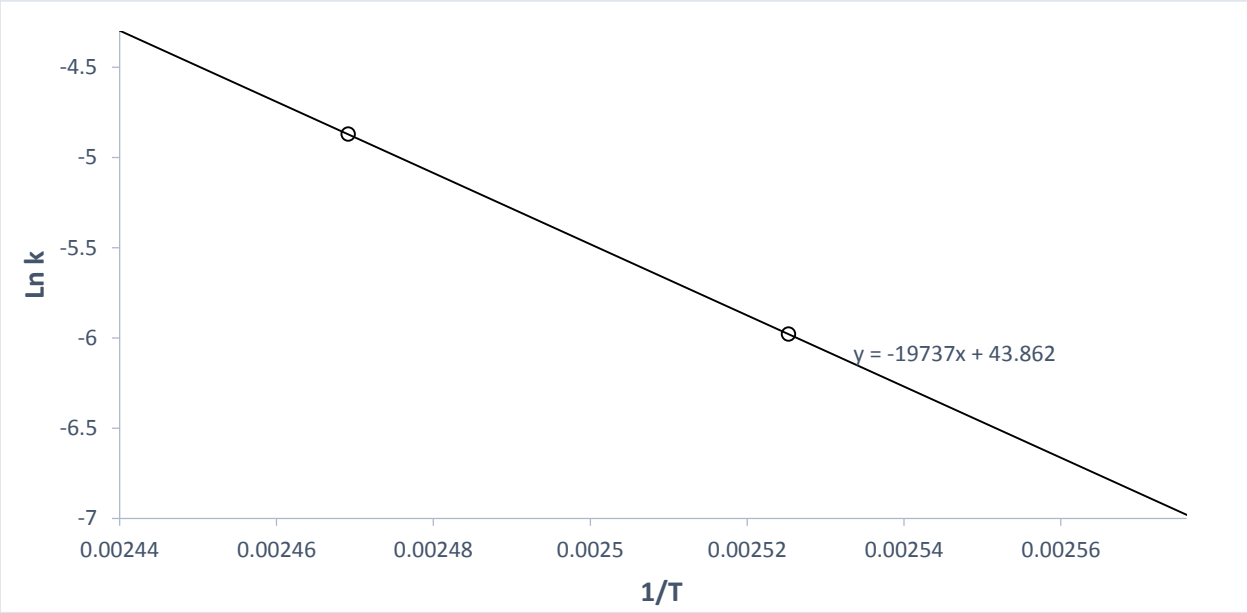

Figure 25: Arrhenius Plot (Xylose).

Due to limited experimental data, confidence intervals cannot be calculated for xylose. Ea was found to be 164.092 J/mol and A was found to be 1.119E+19 ml/(mol.min).

TABLE 13: 2ND ORDER RATE CONSTANTS FOR SUGAR DEHYDRATION AT FIXED TEMPERATURES.

Temperature℃	Rate Constant k [l/(mol.min)]		
	Glucose	Fructose	Xylose
123	4.581E-05	0.007	0.002
132	0.0001	0.018	0.007
144	0.0003	0.045	0.022

We can compare rates of sugar dehydration over the temperature range being studied by observing rate constants. Rate information collected over different temperatures were used to obtain rate constants. From rate constants for each sugar, we are able to generate Arrhenius plots. Since rates need to be compared at a fixed temperature to be of any significance to the comparison, we use the Arrhenius plots to calculate values of k for that temperature. Although limited data were collected at temperatures 123,132 and 141℃ for all sugars, it was possible to calculate rate constants at these temperatures graphically and present them in Table 10. From this table it is clear that lowest rates were seen for glucose dehydration. Fructose dehydration rates were significantly higher.

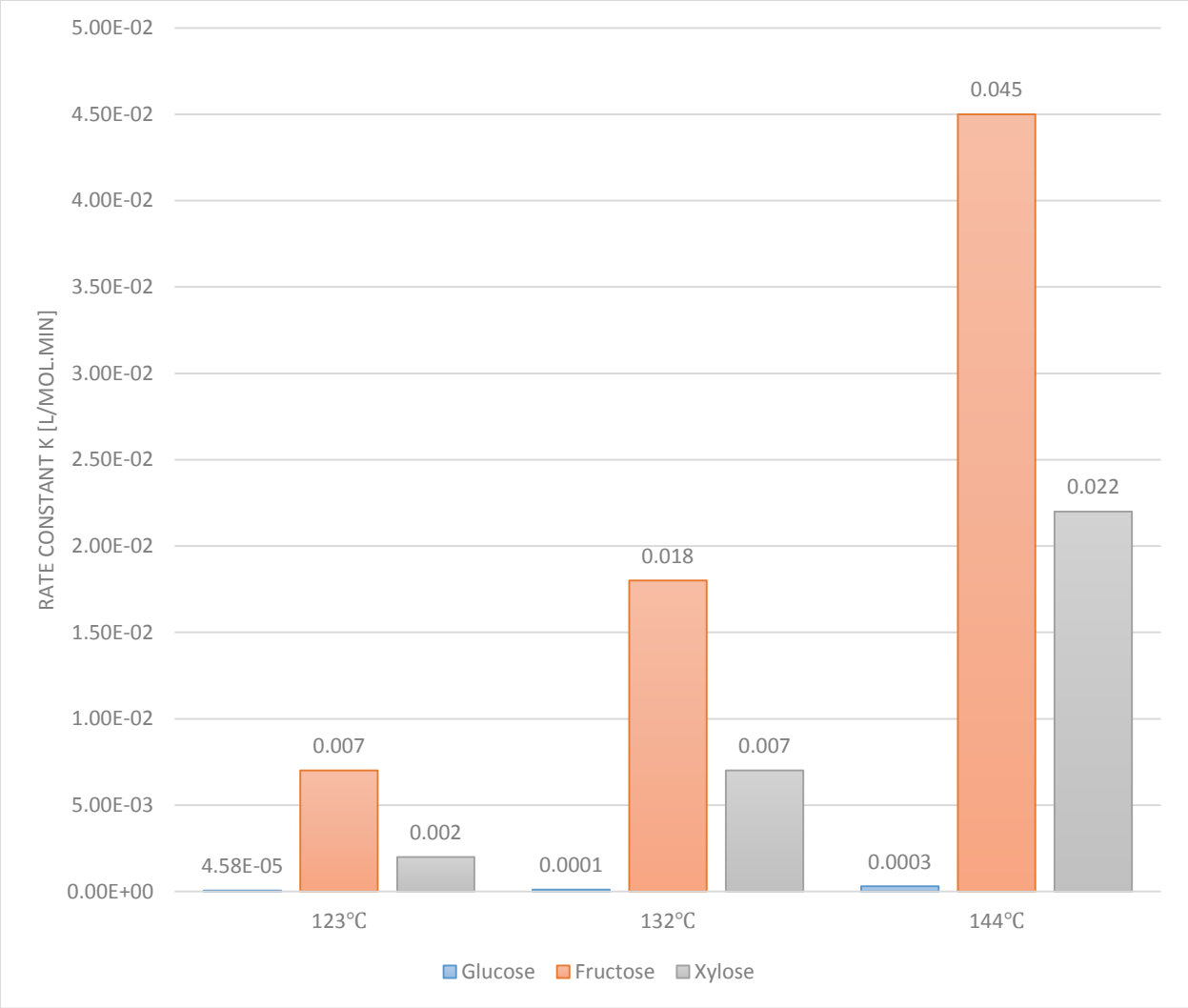

Figure 26: Comparison of sugar dehydration rates based on rate constant. Rate constants taken from Table 10.

Rates of dehydration are found to be greatest for fructose. The large relative rate difference between fructose and glucose have already been explained in previous sections. Xylose, much like fructose and glucose undergo several decomposition reactions at higher temperatures. Dehydration of pentose sugars (xylose) to furfural is different from the mechanisms described for dehydration of hexose sugars (fructose and glucose) to HMF. The intermediate 2, 5-anhydride is formed through the cyclic xylofuranose molecule. Comparison of kinetic parameters

of xylose to the other sugars is difficult owing to the larger confidence intervals in data. Rates of dehydration of xylose are, however greater than glucose as seen in Figure 26. Literature studies that detail xylose dehydration show that the steps leading to anhydride (intermediate) and consequently to furans through the cyclic route are faster than rates seen with open-chain xylose since a very large fraction of open-chains would have to be formed for the reaction at experimental temperatures. Glucose dehydration rates are lowest and rely on isomerization to fructose before forming HMF. Rates as observed (fructose > xylose > glucose) were explained and confirmed in the literature.

Chapter VI

Conclusion and Perspectives

The goal of this project was to develop a method and use it to generate reliable kinetic data for use in industrial applications in the processing of HMF and furfural that have potential as platform chemicals. Reliable data were generated using the reactor built through the systematic heuristics based approach. Special considerations were made to account for changing variables, such as density and its effect on rates. Catalyst loading was quantified based on proton concentration (dissociation dependent on temperature and solvent) and the difference in proton concentration was evaluated. The first part of the work involved designing a system based on literature, assigning convenient and required process/mixing parameters and collecting experimental data. Experimental data were collected between 123 and 141℃. Despite low conversions, rate data were measured for all three sugars. The second part of the study compared the sugars based on the measured and calculated kinetic constants. Higher rates of fructose dehydration as reported in other literature studies were confirmed through the analysis.

Assisting the renewables sector is an important objective of catalysis research. This study explored the use of the homogeneous catalyst sulfuric acid in the dehydration reaction. Similar setups may be used to study alternative catalysts (homogeneous or heterogeneous) and reactions (multiphase). Only research into different catalysts can reveal novel catalysts that are selective, inexpensive to operate and efficient at larger yields.

References

1. Klass, Donald L. *Biomass as a nonfossil fuel source*. No. CONF-790415-P8. American Chemical Society, Washington, DC, 1981.
2. Klass, Donald L. "Biomass for renewable energy and fuels. Encyclopedia of Energy." *Elsevier Inc* 1 (2004): 193-211.
3. Klass, Donald L. *Biomass for renewable energy, fuels, and chemicals*. Academic press, 1998.
4. Klass, D. L., and G. H. Emert. "'Fuels from Biomass and Wastes. Ann Arbor Science." (1981).
5. Wyman, Charles E., et al. "Hydrolysis of cellulose and hemicellulose."*Polysaccharides: Structural diversity and functional versatility* 1 (2005): 1023-1062.
6. Wyman, Charles E., and Norman D. Hinman. "Ethanol." *Applied Biochemistry and Biotechnology* 24.1 (1990): 735-753.
7. Wyman, Charles E. "Ethanol from lignocellulosic biomass: technology, economics, and opportunities." *Bioresource Technology* 50.1 (1994): 3-15.
8. Tyson, Karin Shaine. *Fuel cycle evaluations of biomass-ethanol and reformulated gasoline. Volume 1*. No. NREL/TP--463-4950. National Renewable Energy Lab., Golden, CO (United States); Oak Ridge National Lab., TN (United States); Pacific Northwest Lab., Richland, WA (United States), 1993.
9. Lynd, Lee R., et al. "Fuel ethanol from cellulosic biomass."*Science(Washington)* 251.4999 (1991): 1318-1323.
10. Huber, George W., Sara Iborra, and Avelino Corma. "Synthesis of transportation fuels from biomass: chemistry, catalysts, and engineering."*Chemical reviews* 106.9 (2006): 4044-4098.
11. Lange, Jean-Paul, et al. "Furfural—a promising platform for lignocellulosic biofuels." *ChemSusChem* 5.1 (2012): 150-166.
12. Wang, Tianfu, Michael W. Nolte, and Brent H. Shanks. "Catalytic dehydration of C 6 carbohydrates for the production of hydroxymethylfurfural (HMF) as a versatile platform chemical." *Green Chemistry* 16.2 (2014): 548-572.
13. Phillips, J. R., et al. "Biological production of ethanol from coal synthesis gas."*Applied biochemistry and biotechnology* 39.1 (1993): 559-571.
14. Balat, M. "Mechanisms of thermochemical biomass conversion processes. Part 3: reactions of liquefaction." *Energy Sources, Part A* 30.7 (2008): 649-659.
15. Replace
16. Huber, George W., et al. "Production of liquid alkanes by aqueous-phase processing of biomass-derived carbohydrates." *Science* 308.5727 (2005): 1446-1450.
17. Manzer, Leo E. "Biomass derivatives: a sustainable source of chemicals." *ACS symposium series*. Vol. 921. Oxford University Press, 2006.
18. Perlack, Robert D., et al. *Biomass as feedstock for a bioenergy and bioproducts industry: the technical feasibility of a billion-ton annual supply*. Oak Ridge National Lab TN, 2005.

19. Zakrzewska, Małgorzata E., Ewa Bogel-Łukasik, and Rafał Bogel-Łukasik. "Ionic liquid-mediated formation of 5-hydroxymethylfurfural A promising biomass-derived building block." *Chemical reviews* 111.2 (2010): 397-417.
20. Mosier, Nathan, et al. "Features of promising technologies for pretreatment of lignocellulosic biomass." *Bioresource technology* 96.6 (2005): 673-686.
21. Kobayashi, Hirokazu, and Atsushi Fukuoka. "Synthesis and utilisation of sugar compounds derived from lignocellulosic biomass." *Green Chemistry* 15.7 (2013): 1740-1763.
22. Zakzeski, Joseph, et al. "The catalytic valorization of lignin for the production of renewable chemicals." *Chemical reviews* 110.6 (2010): 3552-3599.
23. Corma, Avelino, Sara Iborra, and Alexandra Velty. "Chemical routes for the transformation of biomass into chemicals." *Chemical Reviews* 107.6 (2007): 2411-2502.
24. Roberts, Virginia, et al. "Towards quantitative catalytic lignin depolymerization."*Chemistry-A European Journal* 17.21 (2011): 5939-5948.
25. Zhao, Chen, et al. "Aqueous-phase hydrodeoxygenation of bio-derived phenols to cycloalkanes." *Journal of Catalysis* 280.1 (2011): 8-16.
26. Azadi, Pooya, et al. "Catalytic conversion of biomass using solvents derived from lignin." *Green Chemistry* 14.6 (2012): 1573-1576.
27. Moreau, Claude, et al. "Selective preparation of furfural from xylose over microporous solid acid catalysts." *Industrial Crops and Products* 7.2 (1998): 95-99.
28. Moreau, Claude, et al. "Dehydration of fructose to 5-hydroxymethylfurfural over H-mordenites." *Applied Catalysis A: General* 145.1 (1996): 211-224.
29. Plow, R. H., et al. "Rotary Digester in Wood Saccharification." *Industrial & Engineering Chemistry* 37.1 (1945): 36-43.
30. Lourvanij, Khavinet, and Gregory L. Rorrer. "Reactions of aqueous glucose solutions over solid-acid Y-zeolite catalyst at 110-160. degree. C." *Industrial & engineering chemistry research* 32.1 (1993): 11-19.
31. Huber, George W., et al. "Production of liquid alkanes by aqueous-phase processing of biomass-derived carbohydrates." *Science* 308.5727 (2005): 1446-1450.
32. Hu, Lei, et al. "Catalytic conversion of biomass-derived carbohydrates into fuels and chemicals via furanic aldehydes." *RSC Advances* 2.30 (2012): 11184-11206.
33. Qian, Xianghong. "Mechanisms and Energetics for Brønsted Acid-Catalyzed Glucose Condensation, Dehydration and Isomerization Reactions." *Topics in Catalysis* 55.3-4 (2012): 218-226.
34. Karinen, Reetta, Kati Vilonen, and Marita Niemelä. "Biorefining: heterogeneously catalyzed reactions of carbohydrates for the production of furfural and hydroxymethylfurfural." *ChemSusChem* 4.8 (2011): 1002-1016.
35. Ståhlberg, Tim, et al. "Synthesis of 5-(Hydroxymethyl) furfural in Ionic Liquids: Paving the Way to Renewable Chemicals." *ChemSusChem* 4.4 (2011): 451-458.
36. Ranoux, Adeline, et al. "5-Hydroxymethylfurfural synthesis from hexoses is autocatalytic." *ACS Catalysis* 3.4 (2013): 760-763.
37. Kuster, B. F. M. "5-Hydroxymethylfurfural (HMF). A review focussing on its manufacture." *Starch-Stärke* 42.8 (1990): 314-321.
38. Alamillo, Ricardo, et al. "The selective hydrogenation of biomass-derived 5-hydroxymethylfurfural using heterogeneous catalysts." *Green Chemistry* 14.5 (2012): 1413-1419.

39. Tong, Xinli, Yang Ma, and Yongdan Li. "Biomass into chemicals: conversion of sugars to furan derivatives by catalytic processes." *Applied Catalysis A: General* 385.1 (2010): 1-13.
40. Román-Leshkov, Yuriy, et al. "Production of dimethylfuran for liquid fuels from biomass-derived carbohydrates." *Nature* 447.7147 (2007): 982-985.
41. Balakrishnan, Madhesan, Eric R. Sacia, and Alexis T. Bell. "Etherification and reductive etherification of 5-(hydroxymethyl) furfural: 5-(alkoxymethyl) furfurals and 2, 5-bis (alkoxymethyl) furans as potential bio-diesel candidates." *Green Chemistry* 14.6 (2012): 1626-1634.
42. Kraus, George A., and Tezcan Guney. "A direct synthesis of 5-alkoxymethylfurfural ethers from fructose via sulfonic acid-functionalized ionic liquids." *Green Chemistry* 14.6 (2012): 1593-1596.
43. Lew, Christopher M., Nafiseh Rajabbeigi, and Michael Tsapatsis. "One-pot synthesis of 5-(ethoxymethyl) furfural from glucose using Sn-BEA and Amberlyst catalysts." *Industrial & Engineering Chemistry Research* 51.14 (2012): 5364-5366.
44. Wang, Tianfu, Michael W. Nolte, and Brent H. Shanks. "Catalytic dehydration of C 6 carbohydrates for the production of hydroxymethylfurfural (HMF) as a versatile platform chemical." *Green Chemistry* 16.2 (2014): 548-572.
45. Hu, Wen-Jing, et al. "Repression of lignin biosynthesis promotes cellulose accumulation and growth in transgenic trees." *Nature biotechnology* 17.8 (1999): 808-812.
46. O'SULLIVAN, ANTOINETTE C. "Cellulose: the structure slowly unravels."*Cellulose* 4.3 (1997): 173-207.
47. Hsu, T. A.; Ladisch, M. R.; Tsao, G. T. *Chem. Technol.* 1980, *10*, 315.
48. Kuster, B. F. M. "5-Hydroxymethylfurfural (HMF). A review focussing on its manufacture." *Starch-Stärke* 42.8 (1990): 314-321.
49. Mosier, Nathan S., Christine M. Ladisch, and Michael R. Ladisch. "Characterization of acid catalytic domains for cellulose hydrolysis and glucose degradation." *Biotechnology and bioengineering* 79.6 (2002): 610-618.
50. Kuster, B. F. M. "5-Hydroxymethylfurfural (HMF). A review focussing on its manufacture." *Starch-Stärke* 42.8 (1990): 314-321.
51. Alonso, David Martin, Jesse Q. Bond, and James A. Dumesic. "Catalytic conversion of biomass to biofuels." *Green Chemistry* 12.9 (2010): 1493-1513.
52. Cinlar, Basak, Tianfu Wang, and Brent H. Shanks. "Kinetics of monosaccharide conversion in the presence of homogeneous Bronsted acids." *Applied Catalysis A: General* 450 (2013): 237-242.
53. Bandura, Andrei V., and Serguei N. Lvov. "The ionization constant of water over wide ranges of temperature and density." *Journal of physical and chemical reference data* 35.1 (2006): 15-30.
54. Marshall, William L., and Ernest V. Jones. "Second Dissociation Constant of Sulfuric Acid from 25 to 350° Evaluated from Solubilities of Calcium Sulfate in Sulfuric Acid Solutions1, 2." *The Journal of Physical Chemistry* 70.12 (1966): 4028-4040.
55. Aristidou, Aristos, and Merja Penttilä. "Metabolic engineering applications to renewable resource utilization." *Current Opinion in Biotechnology* 11.2 (2000): 187-198.
56. Sonderegger, Marco, et al. "Fermentation performance of engineered and evolved xylose-fermenting Saccharomyces cerevisiae strains." *Biotechnology and bioengineering* 87.1 (2004): 90-98.

57. Nandi, R., and S. Sengupta. "Microbial production of hydrogen: an overview."*Critical reviews in microbiology* 24.1 (1998): 61-84.
58. Wyman, Charles E., et al. "Comparative sugar recovery data from laboratory scale application of leading pretreatment technologies to corn stover."*Bioresource technology* 96.18 (2005): 2026-2032.
59. Jambusaria, R. B., and S. P. Potnis. "Bisphenol—Furfural. A High-Temperature Thermosetting Resin." *Polymer Journal* 6.5 (1974): 333-340.
60. Sitthisa, Surapas, Wei An, and Daniel E. Resasco. "Selective conversion of furfural to methylfuran over silica-supported Ni Fe bimetallic catalysts." *Journal of Catalysis* 284.1 (2011): 90-101.
61. Carpita, Nicholas C., and David M. Gibeaut. "Structural models of primary cell walls in flowering plants: consistency of molecular structure with the physical properties of the walls during growth." *The Plant Journal* 3.1 (1993): 1-30.
62. Román-Leshkov, Yuriy, Juben N. Chheda, and James A. Dumesic. "Phase modifiers promote efficient production of hydroxymethylfurfural from fructose."*Science* 312.5782 (2006): 1933-1937.
63. Klingler, D., and H. Vogel. "Influence of process parameters on the hydrothermal decomposition and oxidation of glucose in sub-and supercritical water." *The Journal of Supercritical Fluids* 55.1 (2010): 259-270.
64. Asghari, Feridoun Salak, and Hiroyuki Yoshida. "Dehydration of fructose to 5-hydroxymethylfurfural in sub-critical water over heterogeneous zirconium phosphate catalysts." *Carbohydrate research* 341.14 (2006): 2379-2387.
65. Mosier, Nathan S., et al. "Characterization of dicarboxylic acids for cellulose hydrolysis." *Biotechnology progress* 17.3 (2001): 474-480.
66. Heeres, H. J., L. P. B. M. Janssen, and B. Girisuta. "A Kinetic Study on the Conversion of Glucose to Levulinic Acid." (2006).
67. Van Dam, H. E., A. P. G. Kieboom, and H. Van Bekkum. "The conversion of fructose and glucose in acidic media: formation of hydroxymethylfurfural."*Starch-Stärke* 38.3 (1986): 95-101.
68. Antal, Michael Jerry, William SL Mok, and Geoffrey N. Richards. "Mechanism of formation of 5-(hydroxymethyl)-2-furaldehyde from D-fructose and sucrose."*Carbohydrate research* 199.1 (1990): 91-109.

Vita

Siddharth Bhat

444 Westcott Street, Syracuse, NY 13210 (Authorized to work and ready to relocate without assistance)| E: sibhat@syr.edu | M: (315) 439-7270

EDUCATION

Masters in Chemical Engineering (Current c GPA 3.42/4) ***(Aug 2013-Aug 2015)***

Syracuse University College of Engineering, Syracuse University, Syracuse, New York

Related Coursework: Thermodynamics (Statistical Mechanics) **(4/4),** Biofuels **(4/4),** Chemical Engineering Mathematics (Methods) (**3.33/4**), Green Engineering **(3.67/4),** Drug Delivery **(3.67/4),** Fluid Dynamics, Kinetics **(3.33/4)**, Engineering Statistics **(3.3/4)**.

Bachelors in Chemical Engineering Mumbai University, India. **(Graduation GPA 4/4)** ***(Aug 2009-May 2013)***

EXPERIENCE (2+ years Industrial Experience)

Process Engineer/Laboratory & Manufacturing Liaison, ICM Controls, Syracuse NY ***(Nov 2014-June 2015)***

- Managed on site plating, shadow, etching, water/waste treatment (de-ionized water) for printed circuit board manufacturing process. Conducted Life-Cycle assessments and consequent environmental impact study for all processes.
- Used statistical analysis techniques on data sets acquired from daily spectrometric testing and SEM data to maintain chemical bath concentrations.
- Created, maintained and updated procedural documentation to verify board shop parameters (for ISO 9001:2008 compliance).
- Maintained process safety of staff for ISO, UN, DOT, HAZCOM compliance during operations and chemical shipping. (PSM)
- Performed Mass/Material and energy balances for manufacturing plant to ensure consistent manufacture.
- Applied principles of Lean Six Sigma and Statistics to reduce Manufacturing Downtime.
- Operated and maintained filter presses and waste water treatment for over 50,000 gallons.
- Reduced overall metallic copper waste by recommending and assisting installation of on-site recovery system (UN certified).
- Conversant in CAPA, HAZOP, LOPA, Event tree analysis and root cause approaches to troubleshooting.

Process Engineer / Research Intern, Trilok Fabrication Corporation, (Mumbai) India ***(May 2012-Aug 2013)***

- Assisted a team in building high gravity contactors to replace traditional Amine Gas Separators in Petroleum Industry. (Hindustan Petroleum)
- Used patented Ramshaw's process and modified patented D.P. Rao's process to enhance effective operating interfacial area and reaction area by overcoming reaction resistances.
- Maintained **100 g's** for increased capabilities, increased throughputs by **5-10** times, reduced size by a factor of **100.**
- Enhanced Mass transfer and reduced emissions by increasing Liquid Side mass transfer by **3-9** times.

Research Assistant, Syracuse University, Syracuse, NY ***(Jan 2014 – Aug 2015)***

- Certification: OSHA'S Laboratory Training (29 CFR 1910.1450)
- Performed background study and experimental setup procedures (Chemical Engineering Heuristics)
- Problem/Error isolation and Troubleshooting/Diagnostics
- Designed systems for data collection and analysis and interpretation of data using analytical and computational tools
- Conversant in the use of lab equipment (HPLC UV-IR Spectroscope, Mass Spec., Temp. Control, FTIR, GC, FID, Pumps, Swage NPT Fittings.)

ACADEMIC PROJECTS

Thesis Work, Syracuse University, Catalysis lab (Advisor: Jesse.Q.Bond) ***(Aug 2014-Aug 2015)***

- Thesis title "Study of Homogeneous Mineral Acid Dehydration of Monosaccharides in a CSTR"
- Developed a process to improve kinetics and scale-up production of Alternative Fuel Intermediates
- Accomplished Application of Heuristics for Construction of Continuous Stirred Tank Reactor.
- Studied compatibility and properties of materials (Mechanical/Chemical) (SS 316, PTFE, PFA, Ceramics, Glass)
- Conducted Material balances using UV/RI chromatograms. Gathered Mixing data using a series of tracer experiments.

Thermodynamics and Statistical Mechanics to Explain Colors of Nebulae (Hubble Satellite Images) ***(2013-2014)***

- Used concepts of Spectroscopy and molecular/atomic partition functions to arrive at wavelength relations.

Green manufacturing practices and alternative processes for p-Xylene Production ***(2013-2014)***

- Conducted a Study of reaction kinetics, PFD, Hazard Identification and Prevention mechanisms, Exposure & Emission Calculations, Suggested modifications, Life-cycle assessments. (Following EPA conventions and guidelines)

Simulation of the dynamic freeze drying process using COMSOL^{tm} ***(2013-2014)***

- Simulated dynamic environments, selection criteria for geometry of study medium, Mathematical mesh convergence, illustration of fluid transport, diffusion, heat transfer, Special case non-linear behavior.

Recovery of Sulfur from Acid Gas, Essar Petroleum Refinery, Jamnagar. (Mumbai University) ***(2012-2013)***

- Completed Physical & Economic Evaluation, Comparison to alternatives, PFD P&ID draft, Calculations, Market Survey, Equipment study

SEMINARS CONDUCTED

Advanced Engineering Ceramics (Researched and presented on origin of ceramics, Traditional Ceramics, Advanced Classification, Properties, Manufacturing Processes) ***(Feb-2013)***

Advances in Food Processing Technology (Studied crushers, driers, mechanical separators, Freeze driers, associated food processing) ***(Sep-2012)***

TECHNICAL SKILLS

- **Software Applications and Simulation Tools:** MS Office, TANKS (EPA), EPISUITE, AutoCAD, MedChem (Molecular Models), Adobe Suite, ASPEN PLUS, UniSim ^{tm}, Comsol ^{tm}, Matlab, Polymath, Minitab.

LEADERSHIP EXPERIENCE/AWARDS

Managed and hosted Programs for the IICHE (Indian Institute of Chemical Engineers). (Mumbai) ***(2012-2013)***

Received a 50% academic tuition grant from Syracuse University. ***(2013-2015)***